SLAC–PUB–8627
September 2000

The Light-Cone Fock Expansion in Quantum Chromodynamics *

Stanley J. Brodsky
Stanford Linear Accelerator Center
Stanford University, Stanford, California 94309
E-mail: sjbth@slac.stanford.edu

Abstract

A fundamental question in QCD is the non-perturbative structure of hadrons at the amplitude level—not just the single-particle flavor, momentum, and helicity distributions of the quark constituents, but also the multi-quark, gluonic, and hidden-color correlations intrinsic to hadronic and nuclear wavefunctions. The light-cone Fock-state representation of QCD encodes the properties of a hadrons in terms of frame-independent wavefunctions. A number of applications are discussed, including semileptonic B decays, deeply virtual Compton scattering, and dynamical higher twist effects in inclusive reactions. A new type of jet production reaction, "self-resolving diffractive interactions" can provide direct information on the light-cone wavefunctions of hadrons in terms of their quark and gluon degrees of freedom as well as the composition of nuclei in terms of their nucleon and mesonic degrees of freedom. The relation of the intrinsic sea to the light-cone wavefunctions is discussed. The physics of light-cone wavefunctions is illustrated for the quantum fluctuations of an electron.

Presented at
VII HADRON PHYSICS 2000
Caraguatatuba, São Paulo, Brazil
April 10–15, 2000

*Work supported by Department of Energy contract DE–AC03–76SF00515.

1 Introduction

Quantum Chromodynamics, the non-abelian $SU(N_C = 3)$ gauge theory of quark and gluons is the central theory of particle and nuclear physics. The range of applications of QCD to physical processes is extraordinary, ranging from the dynamics and structure of hadrons and nuclei, the properties of electroweak transitions, quark and gluon jet processes, to the properties and phases of hadronic matter at the earliest stages of the universe. At very short distances QCD is believed to unify with the electroweak interactions, and possibly even gravity, into more fundamental theories.

There has been enormous progress in understanding QCD since its inception in 1973,[1] particularly in the applications of the perturbative theory to inclusive and exclusive processes involving collisions at large momentum transfer. New experimental tools are continually being developed which probe the non-perturbative structure of the theory, such as hard diffractive reactions, self-resolving jet reactions, semi-exclusive reactions, deeply virtual Compton scattering, and heavy ion collisions. Nevertheless, many fundamental questions have not been resolved. These include rigorous proofs of color confinement, the behavior of the QCD coupling at small scales, the computation of the non-perturbative structure of hadrons in terms of their quark and gluon degrees of freedom, the problem of $n!$ growth of the perturbation theory (renormalon phenomena), the nature of the pomeron and reggeons, the nature of shadowing and antishadowing in nuclear collisions, the apparent conflict between QCD vacuum structure and the small size of the cosmological constant, and the problems of scale and scheme ambiguities in perturbative QCD expansion. One of the most pressing problems is to understand the QCD physics of exclusive B-meson decays at the amplitude level, since the interpretation of the basic parameters of the electroweak theory and CP violation depend on hadronic dynamics and phase structure.

The most challenging nonperturbative problem in QCD is the solution of the bound state problem; *i.e.*, to determine the structure and spectrum of hadrons and nuclei in terms of their quark and gluon degrees of freedom. Ideally, one wants a frame-independent, quantum-mechanical description of hadrons at the amplitude level capable of encoding multi-quark, hidden-color and gluon momentum, helicity, and flavor correlations in the form of universal process-independent hadron wavefunctions. Remarkably, the light-cone Fock expansion allows just such a unifying representation.

Formally, the light-cone expansion is constructed by quantizing QCD at fixed light-cone time [2] $\tau = t + z/c$ and forming the invariant light-cone Hamiltonian: $H_{LC}^{QCD} = P^+P^- - \vec{P}_\perp^2$ where $P^\pm = P^0 \pm P^z$.[3] The operator $P^- = i\frac{d}{d\tau}$ generates light-cone time translations. The P^+ and $\vec{P}_\perp$ momentum operators are independent of the interactions. Each intermediate state consists of particles with light-cone energy $k^- = \frac{\vec{k}_\perp^2 + m^2}{k^+} > 0$ and positive k^+.

The procedure for quantizing non-Abelian gauge theory in QCD is well-known.[4, 5] In brief: if one chooses light-cone gauge $A^+ = 0$, the dependent gauge field A^- and quark field $\psi^- = \Lambda^-\psi$ can be eliminated in terms of the physical transverse field

$A^\perp$ and $A^+ = \Lambda^+\psi$ fields. Here $\Lambda^\pm = \frac{1}{2}\gamma^\mp\gamma^\pm$ are hermitian projection operators. Remarkably, no ghosts fields appear in the formalism, since only physical degrees of freedom propagate. The interaction Hamiltonian includes the usual Dirac interactions between the quarks and gluons, the three-point and four-point gluon non-Abelian interactions plus instantaneous [5] light-cone time gluon exchange and quark exchange contributions:

$$\begin{aligned}\mathcal{H}_{int} = & -g\,\overline{\psi}^i\gamma^\mu A_\mu{}^{ij}\psi^j \\ & +\frac{g}{2}\,f^{abc}\,(\partial_\mu A^a{}_\nu - \partial_\nu A^a{}_\mu)A^{b\mu}A^{c\nu} \\ & +\frac{g^2}{4}\,f^{abc}f^{ade}A_{b\mu}A^{d\mu}A_{c\nu}A^{e\nu} \\ & -\frac{g^2}{2}\,\overline{\psi}^i\gamma^+\,(\gamma^{\perp'}A_{\perp'})^{ij}\,\frac{1}{i\partial_-}\,(\gamma^\perp A_\perp)^{jk}\,\psi^k \\ & -\frac{g^2}{2}\,j^+{}_a\,\frac{1}{(\partial_-)^2}\,j^+{}_a \end{aligned} \tag{1}$$

where

$$j^+{}_a = \overline{\psi}^i\gamma^+(t_a)^{ij}\psi^j + f_{abc}(\partial_- A_{b\mu})A^{c\mu} \tag{2}$$

Srivastava and I have recently shown how one can use the Dyson-Wick formalism to construct the Feynman rules in light-cone gauge for QCD. The gauge fields satisfy both the light-cone gauge and the Lorentz condition $\partial_\mu A^\mu = 0$. We have also shown that one can also effectively quantize QCD in the covariant Feynman gauge.[6]

The eigen-spectrum of H_{LC}^{QCD} in principle gives the entire mass squared spectrum of color-singlet hadron states in QCD, together with their respective light-cone wavefunctions. For example, the proton state satisfies: $H_{LC}^{QCD}|\,\Psi_p\rangle = M_p^2|\,\Psi_p\rangle$. The projection of the proton's eigensolution $|\,\Psi_p\rangle$ on the color-singlet $B = 1$, $Q = 1$ eigenstates $\{|\,n\rangle\}$ of the free Hamiltonian $H_{LC}^{QCD}(g = 0)$ gives the light-cone Fock expansion: [7]

$$\begin{aligned}\Big|\Psi_p; P^+, \vec{P}_\perp, \lambda\Big\rangle = & \sum_{n\geq 3,\lambda_i}\int \Pi_{i=1}^n \frac{d^2k_{\perp i}dx_i}{\sqrt{x_i}16\pi^3} \\ & 16\pi^3\delta\left(1-\sum_j^n x_j\right)\delta^{(2)}\left(\sum_\ell^n \vec{k}_{\perp\ell}\right) \\ & \Big|n; x_iP^+, x_i\vec{P}_\perp + \vec{k}_{\perp i}, \lambda_i\Big\rangle\,\psi_{n/p}(x_i, \vec{k}_{\perp i}, \lambda_i).\end{aligned}$$

The light-cone Fock wavefunctions $\psi_{n/H}(x_i, \vec{k}_{\perp i}, \lambda_i)$ thus interpolate between the hadron H and its quark and gluon degrees of freedom. The light-cone momentum fractions of the constituents, $x_i = k_i^+/P^+$ with $\sum_{i=1}^n x_i = 1$, and the transverse momenta $\vec{k}_{\perp i}$ with $\sum_{i=1}^n \vec{k}_{\perp i} = \vec{0}_\perp$ appear as the momentum coordinates of the light-cone Fock wavefunctions. A crucial feature is the frame-independence of the light-cone wavefunctions.

The x_i and $\vec{k}_{\perp i}$ are relative coordinates independent of the hadron's momentum P^μ. The actual physical transverse momenta are $\vec{p}_{\perp i} = x_i \vec{P}_\perp + \vec{k}_{\perp i}$.

The λ_i label the light-cone spin S^z projections of the quarks and gluons along the z direction. The physical gluon polarization vectors $\epsilon^\mu(k,\ \lambda = \pm 1)$ are specified in light-cone gauge by the conditions $k \cdot \epsilon = 0,\ \eta \cdot \epsilon = \epsilon^+ = 0$. Each light-cone Fock wavefunction satisfies conservation of the z projection of angular momentum: $J^z = \sum_{i=1}^n S_i^z + \sum_{j=1}^{n-1} l_j^z$. The sum over S_i^z represents the contribution of the intrinsic spins of the n Fock state constituents. The sum over orbital angular momenta $l_j^z = -\mathrm{i}(k_j^1 \frac{\partial}{\partial k_j^2} - k_j^2 \frac{\partial}{\partial k_j^1})$ derives from the $n-1$ relative momenta. This excludes the contribution to the orbital angular momentum due to the motion of the center of mass, which is not an intrinsic property of the hadron.[8]

Light-cone wavefunctions are thus the frame-independent interpolating functions between hadron and quark and gluon degrees of freedom. Hadron amplitudes are computed from the convolution of the light-cone wavefunctions with irreducible quark-gluon amplitudes. For example, space-like form factors can be represented as the diagonal $\Delta n = 0$ overlap of light-cone wavefunctions. Time-like form factors such as semi-exclusive B decays can be expressed as the sum of diagonal $\Delta n = 0$ and $\Delta n = 2$ overlap integrals. Structure functions are simply related to the sum over absolute squares of the light-cone wavefunctions. More generally, all multi-quark and gluon correlations in the bound state are represented by the light-cone wavefunctions. Thus in principle, all of the complexity of a hadron is encoded in the light-cone Fock representation, and the light-cone Fock representation is thus a representation of the underlying quantum field theory.

The LC wavefunctions $\psi_{n/H}(x_i, \vec{k}_{\perp i}, \lambda_i)$ are universal, process-independent, and thus control all hadronic reactions. In the case of deep inelastic scattering, one needs to evaluate the imaginary part of the virtual Compton amplitude $\mathcal{M}[\gamma^*(q)p \to \gamma^*(q)p]$. The simplest frame choice for electroproduction is $q^+ = 0, q_\perp^2 = Q^2 = -q^2, q^- = 2q \cdot p/P^+, p^+ = P^+, p_\perp = 0_\perp, p^- = M_p^2/P^+$. At leading twist, soft final-state interactions of the outgoing hard quark line are power-law suppressed in light-cone gauge, so the calculation of the virtual Compton amplitude reduces to the evaluation of matrix elements of the products of free quark currents of the free quarks. The absorptive amplitude imposes conservation of light-cone energy: $p^- + q^- = \sum_i^n k_i^-$ for the $n-$particle Fock state. In the impulse approximation, where only one quark q recoils against the scattered lepton, this condition becomes

$$M_p^2 + 2q \cdot p = \frac{(\vec{k}_{\perp q} + \vec{q}_\perp)^2 + m_q^2}{x_q} + \sum_{i \neq q} \frac{k_{\perp i}^2 + m_i^2}{x_i} \ . \tag{3}$$

If we neglect the transverse momenta $k_\perp^2$ relative to Q^2 in the Bjorken limit $Q^2 \to \infty$, $x_{bj} = Q^2/2q \cdot p$ fixed, we obtain the condition $x_q = x_{bj}$; *i.e.*, the light-cone fraction $x_q = k^+/p^+$ of the struck quark is kinematically fixed to be equal to the Bjorken ratio. Contributions from high $k_\perp^2 = \mathcal{O}(Q^2)$ which originate from the perturbative

QCD radiative corrections to the struck quark line lead to the DGLAP evolution equations.

Thus given the light-cone wavefunctions, one can compute[4] all of the leading twist helicity and transversity distributions measured in polarized deep inelastic lepton scattering.[9] For example, the helicity-specific quark distributions at resolution Λ correspond to

$$q_{\lambda_q/\Lambda_p}(x,\Lambda) = \sum_{n,q_a} \int \prod_{j=1}^{n} \frac{dx_j d^2 k_{\perp j}}{16\pi^3} \sum_{\lambda_i} |\psi^{(\Lambda)}_{n/H}(x_i, \vec{k}_{\perp i}, \lambda_i)|^2 \tag{4}$$
$$\times 16\pi^3 \delta\left(1 - \sum_i^n x_i\right) \delta^{(2)}\left(\sum_i^n \vec{k}_{\perp i}\right) \delta(x - x_q) \delta_{\lambda,\lambda_q} \Theta(\Lambda^2 - \mathcal{M}_n^2) \ ,$$

where the sum is over all quarks q_a which match the quantum numbers, light-cone momentum fraction x, and helicity of the struck quark. Similarly, the transversity distributions and off-diagonal helicity convolutions are defined as a density matrix of the light-cone wavefunctions. This defines the LC factorization scheme [4] where the invariant mass squared $\mathcal{M}_n^2 = \sum_{i=1}^n (k_{\perp i}^2 + m_i^2)/x_i$ of the n partons of the light-cone wavefunctions are limited to $\mathcal{M}_n^2 < \Lambda^2$

The light-cone wavefunctions also specify the multi-quark and gluon correlations of the hadron. For example, the distribution of spectator particles in the final state which could be measured in the proton fragmentation region in deep inelastic scattering at an electron-proton collider are in principle encoded in the light-cone wavefunctions. We also note that the high momentum tail of the light-cone wavefunctions can be computed perturbatively in QCD. In particular, the evolution equations for structure functions and distribution amplitudes follow from the perturbative high transverse momentum behavior of the light-cone wavefunctions.[7] The gauge theory features of color transparency and color opacity for color singlet hadrons follows from the distribution of the quarks and gluons in transverse space of the hadron wavefunctions.[10]

There are many sources of power-law corrections to the standard leading twist formula for deep inelastic structure functions. Higher-twist corrections arise from QCD radiative corrections (renormalons), final-state interactions, finite target mass effects [11], constituent masses, and their transverse momenta $k_\perp$.[12] Despite the many sources of power-law corrections to the deep inelastic cross section, certain types of dynamical contributions will stand out at large x_{bj} since they arise from compact, highly-correlated fluctuations of the proton wavefunction. In particular, as I will discuss in Section 12, there are particularly interesting dynamical $\mathcal{O}(1/Q^2)$ corrections which are due to the *interference* of quark currents; *i.e.*, contributions which involve leptons scattering amplitudes from two different quarks.

Recently, the E791 experiment at Fermilab has demonstrated that the light-cone wavefunction of a hadron can be directly measured by diffractively dissociating a high energy hadron into jets.[13] I will review the physics of self-resolving interactions in Section 12.

In addition to the light-cone Fock expansion, a number of other useful theoretical tools are available to eliminate theoretical ambiguities in QCD predictions:

(1) Conformal symmetry provides a template for QCD predictions,[20] leading to relations between observables which are present even in a theory which is not scale invariant. For example, the natural representation of distribution amplitudes is in terms of an expansion of orthonormal conformal functions multiplied by anomalous dimensions determined by QCD evolution equations.[14, 15, 16] Thus an important guide in QCD analyses is to identify the underlying conformal relations of QCD which are manifest if we drop quark masses and effects due to the running of the QCD couplings. In fact, if QCD has an infrared fixed point (vanishing of the Gell Mann-Low function at low momenta), the theory will closely resemble a scale-free conformally symmetric theory in many applications.

(2) Commensurate scale relations[17, 18] are perturbative QCD predictions which relate observable to observable at fixed relative scale, such as the "generalized Crewther relation" [19], which connects the Bjorken and Gross-Llewellyn Smith deep inelastic scattering sum rules to measurements of the e^+e^- annihilation cross section. The relations have no renormalization scale or scheme ambiguity. The coefficients in the perturbative series for commensurate scale relations are identical to those of conformal QCD; thus no infrared renormalons are present.[20] One can identify the required conformal coefficients at any finite order by expanding the coefficients of the usual PQCD expansion around a formal infrared fixed point, as in the Banks-Zak method.[21] All non-conformal effects are absorbed by fixing the ratio of the respective momentum transfer and energy scales. In the case of fixed-point theories, commensurate scale relations relate both the ratio of couplings and the ratio of scales as the fixed point is approached. [20]

(3) α_V and Skeleton Schemes. A physically natural scheme for defining the QCD coupling in exclusive and other processes is the $\alpha_V(Q^2)$ scheme defined from the potential of static heavy quarks. Heavy-quark lattice gauge theory can provide highly precise values for the coupling. All vacuum polarization corrections due to fermion pairs are then automatically and analytically incorporated into the Gell Mann-Low function, thus avoiding the problem of explicitly computing and resumming quark mass corrections related to the running of the coupling.[22] The use of a finite effective charge such as α_V as the expansion parameter also provides a basis for regulating the infrared nonperturbative domain of the QCD coupling. A similar coupling and scheme can be based on an assumed skeleton expansion of the theory.[21]

(4) The Abelian Correspondence Principle. One can consider QCD predictions as analytic functions of the number of colors N_C and flavors N_F. In particular, one can show at all orders of perturbation theory that PQCD predictions reduce to those of an Abelian theory at $N_C \to 0$ with $\widehat{\alpha} = C_F \alpha_s$ and $\widehat{N}_F = N_F/TC_F$ held fixed.[23] There is thus a deep connection between QCD processes and their corresponding QED analogs.

A review of these topics can be found in the lectures by Rathsman and myself. [24, 20]

2 Applications of Light-cone wavefunctions to Current Matrix Elements

As I shall review in the next sections, the light-cone Fock representation of current matrix elements has a number of simplifying properties. Matrix elements of space-like local operators for the coupling of photons, gravitons and the deep inelastic structure functions can all be expressed as overlaps of light-cone wavefunctions with the same number of Fock constituents. This is possible since one can choose the special frame $q^+ = 0$ [25, 26] for space-like momentum transfer and take matrix elements of "plus" components of currents such as J^+ and T^{++}. Since the physical vacuum in light-cone quantization coincides with the perturbative vacuum, no contributions to matrix elements from vacuum fluctuations occur.[27] Exclusive semi-leptonic B-decay amplitudes involving time-like currents such as $B \to A\ell\overline{\nu}$ can also be evaluated exactly.[28, 29] In this case, the time-like decay matrix elements require the computation of both the diagonal matrix element $n \to n$ where parton number is conserved and the off-diagonal $n+1 \to n-1$ convolution such that the current operator annihilates a $q\overline{q'}$ pair in the initial B wavefunction. This term is a consequence of the fact that the time-like decay $q^2 = (p_\ell + p_{\overline{\nu}})^2 > 0$ requires a positive light-cone momentum fraction $q^+ > 0$. A similar result holds for the light-cone wavefunction representation of the deeply virtual Compton amplitude.[30]

3 Electromagnetic and Gravitational Form Factors

The light-cone Fock representation allows one to compute all matrix elements of local currents as overlap integrals of the light-cone Fock wavefunctions. In particular, we can evaluate forward and non-forward matrix elements of the electroweak currents, moments of the deep inelastic structure functions, as well as the electromagnetic form factors and the magnetic moment. Given the local operators for the energy-momentum tensor $T^{\mu\nu}(x)$ and the angular momentum tensor $M^{\mu\nu\lambda}(x)$, one can directly compute momentum fractions, spin properties, the gravitomagnetic moment, and the form factors $A(q^2)$ and $B(q^2)$ appearing in the coupling of gravitons to composite systems.

In the case of a spin-$\frac{1}{2}$ composite system, the Dirac and Pauli form factors $F_1(q^2)$ and $F_2(q^2)$ are defined by

$$\langle P'|J^\mu(0)|P\rangle = \overline{u}(P')\left[F_1(q^2)\gamma^\mu + F_2(q^2)\frac{i}{2M}\sigma^{\mu\alpha}q_\alpha\right]u(P) \ , \tag{5}$$

where $q^\mu = (P'-P)^\mu$ and $u(P)$ is the bound state spinor. In the light-cone formalism it is convenient to identify the Dirac and Pauli form factors from the helicity-conserving and helicity-flip vector current matrix elements of the J^+ current [31]:

$$\left\langle P+q,\uparrow \left| \frac{J^+(0)}{2P^+} \right| P,\uparrow \right\rangle = F_1(q^2) \ , \tag{6}$$

$$\left\langle P+q,\uparrow \left| \frac{J^+(0)}{2P^+} \right| P,\downarrow \right\rangle = -(q^1 - \mathrm{i}q^2)\frac{F_2(q^2)}{2M} \ . \tag{7}$$

The magnetic moment of a composite system is one of its most basic properties. The magnetic moment is defined at the $q^2 \to 0$ limit,

$$\mu = \frac{e}{2M}\left[F_1(0) + F_2(0)\right], \tag{8}$$

where e is the charge and M is the mass of the composite system. We use the standard light-cone frame ($q^\pm = q^0 \pm q^3$):

$$\begin{aligned} q &= (q^+, q^-, \vec{q}_\perp) = \left(0, \frac{-q^2}{P^+}, \vec{q}_\perp\right), \\ P &= (P^+, P^-, \vec{P}_\perp) = \left(P^+, \frac{M^2}{P^+}, \vec{0}_\perp\right), \end{aligned} \tag{9}$$

where $q^2 = -2P\cdot q = -\vec{q}_\perp^2$ is 4-momentum square transferred by the photon.

The Pauli form factor and the anomalous magnetic moment $\kappa = \frac{e}{2M}F_2(0)$ can then be calculated from the expression

$$-(q^1 - \mathrm{i}q^2)\frac{F_2(q^2)}{2M} = \sum_a \int \frac{\mathrm{d}^2\vec{k}_\perp \mathrm{d}x}{16\pi^3} \sum_j e_j \ \psi_a^{\uparrow *}(x_i, \vec{k}'_{\perp i}, \lambda_i)\, \psi_a^{\downarrow}(x_i, \vec{k}_{\perp i}, \lambda_i) \ , \tag{10}$$

where the summation is over all contributing Fock states a and struck constituent charges e_j. The arguments of the final-state light-cone wavefunction are [32, 26]

$$\vec{k}'_{\perp i} = \vec{k}_{\perp i} + (1 - x_i)\vec{q}_\perp \tag{11}$$

for the struck constituent and

$$\vec{k}'_{\perp i} = \vec{k}_{\perp i} - x_i\vec{q}_\perp \tag{12}$$

for each spectator. Notice that the magnetic moment must be calculated from the spin-flip non-forward matrix element of the current. It is not given by a diagonal forward matrix element.[33] In the ultra-relativistic limit where the radius of the system is small compared to its Compton scale $1/M$, the anomalous magnetic moment must vanish.[34] The light-cone formalism is consistent with this theorem.

The form factors of the energy-momentum tensor for a spin-$\frac{1}{2}$ composite are defined by

$$\begin{aligned} \langle P'|T^{\mu\nu}(0)|P\rangle = \overline{u}(P')\Big[& A(q^2)\gamma^{(\mu}\overline{P}^{\nu)} + B(q^2)\frac{i}{2M}\overline{P}^{(\mu}\sigma^{\nu)\alpha}q_\alpha \\ & + C(q^2)\frac{1}{M}(q^\mu q^\nu - g^{\mu\nu}q^2)\Big]\, u(P) \ , \end{aligned} \tag{13}$$

where $q^\mu = (P' - P)^\mu$, $\overline{P}^\mu = \frac{1}{2}(P' + P)^\mu$, $a^{(\mu}b^{\nu)} = \frac{1}{2}(a^\mu b^\nu + a^\nu b^\mu)$, and $u(P)$ is the spinor of the system.

As in the light-cone decomposition Eqs. (6) and (7) of the Dirac and Pauli form factors for the vector current [31], we can obtain the light-cone representation of the $A(q^2)$ and $B(q^2)$ form factors of the energy-tensor Eq. (13). Since we work in the interaction picture, only the non-interacting parts of the energy momentum tensor $T^{++}(0)$ need to be computed in the light-cone formalism. By calculating the $++$ component of Eq. (13), we find

$$\left\langle P+q,\uparrow \left| \frac{T^{++}(0)}{2(P^+)^2} \right| P,\uparrow \right\rangle = A(q^2) \ , \tag{14}$$

$$\left\langle P+q,\uparrow \left| \frac{T^{++}(0)}{2(P^+)^2} \right| P,\downarrow \right\rangle = -(q^1 - \mathrm{i}q^2)\frac{B(q^2)}{2M} \ . \tag{15}$$

The $A(q^2)$ and $B(q^2)$ form factors Eqs. (14) and (15) are similar to the $F_1(q^2)$ and $F_2(q^2)$ form factors Eqs. (6) and (7) with an additional factor of the light-cone momentum fraction $x = k^+/P^+$ of the struck constituent in the integrand. The $B(q^2)$ form factor is obtained from the non-forward spin-flip amplitude. The value of $B(0)$ is obtained in the $q^2 \to 0$ limit. The angular momentum projection of a state is given by

$$\left\langle J^i \right\rangle = \frac{1}{2}\epsilon^{ijk} \int d^3x \left\langle T^{0k}x^j - T^{0j}x^k \right\rangle = A(0)\left\langle L^i \right\rangle + [A(0)+B(0)]\,\overline{u}(P)\frac{1}{2}\sigma^i u(P) \ . \tag{16}$$

This result is derived using a wave-packet description of the state. The $\langle L^i \rangle$ term is the orbital angular momentum of the center of mass motion with respect to an arbitrary origin and can be dropped. The coefficient of the $\langle L^i \rangle$ term must be 1; $A(0) = 1$ also follows when we evaluate the four-momentum expectation value $\langle P^\mu \rangle$. Thus the total intrinsic angular momentum J^z of a nucleon can be identified with the values of the form factors $A(q^2)$ and $B(q^2)$ at $q^2 = 0$:

$$\langle J^z \rangle = \left\langle \frac{1}{2}\sigma^z \right\rangle [A(0)+B(0)] \ . \tag{17}$$

One can define individual quark and gluon contributions to the total angular momentum from the matrix elements of the energy momentum tensor.[35] However, this definition is only formal; $A_{q,g}(0)$ can be interpreted as the light-cone momentum fraction carried by the quarks or gluons $\langle x_{q,g} \rangle$. The contributions from $B_{q,g}(0)$ to J_z cancel in the sum. In fact, it will be shown below [8] that the contributions to $B(0)$ vanish when summed over the constituents of each individual Fock state.

We will give an explicit realization of these relations in the light-cone Fock representation for general composite systems. In the next section we will illustrate the formulae by computing the electron's electromagnetic and energy-momentum tensor form factors to one-loop order in QED. In fact, the structure of this calculation has much more generality and can be used as a template for more general composite systems.

4 The Light-Cone Fock State Decomposition and Spin Structure of Leptons in QED

Recently Dae Sung Hwang, Bo-Qiang Ma, Ivan Schmidt, and I [8] have shown that the light-cone wavefunctions generated by the radiative corrections to the electron in QED provides a simple system for understanding the spin and angular momentum decomposition of relativistic systems. This perturbative model also illustrates the interconnections between Fock states of different number. The model is patterned after the quantum structure which occurs in the one-loop Schwinger $\alpha/2\pi$ correction to the electron magnetic moment.[36] In effect, we can represent a spin-$\frac{1}{2}$ system as a composite of a spin-$\frac{1}{2}$ fermion and spin-one vector boson with arbitrary masses. A similar model has been used to illustrate the matrix elements and evolution of light-cone helicity and orbital angular momentum operators.[37] This representation of a composite system is particularly useful because it is based on two constituents but yet is totally relativistic. We can then explicitly compute the form factors $F_1(q^2)$ and $F_2(q^2)$ of the electromagnetic current, and the various contributions to the form factors $A(q^2)$ and $B(q^2)$ of the energy-momentum tensor. The anomalous moment coupling $B(0)$ to a graviton is shown to vanish for any composite system. This remarkable result, first derived by Okun and Kobzarev, [38, 39, 40, 41, 42] is shown to follow directly from the Lorentz boost properties of the light-cone Fock representation.[8]

The Schwinger one-loop radiative correction to the electron current in quantum electrodynamics has played a historic role in the development of quantum field theory. In the language of light-cone quantization, the electron anomalous magnetic moment $a_e = \alpha/2\pi$ is due to the one-fermion one-gauge boson Fock state component of the physical electron. An explicit calculation of the anomalous moment in this framework was given by Brodsky and Drell.[31] We shall show here that the light-cone wavefunctions of the electron provides an ideal system to check explicitly the intricacies of spin and angular momentum in quantum field theory. In particular, we shall evaluate the matrix elements of the QED energy momentum tensor and show how the "spin crisis" is resolved in QED for an actual physical system. The analysis is exact in perturbation theory. The same method can be applied to the moments of structure functions and the evaluation of other local matrix elements. We will also show how the perturbative light-cone wavefunctions of leptons and photons provide a template for the wavefunctions of non-perturbative composite systems resembling hadrons in QCD.

The light-cone Fock state wavefunctions of an electron can be systematically evaluated in QED. The QED Lagrangian density is

$$\mathcal{L} = \frac{i}{2}\ [\ \overline{\psi}\gamma^\mu(\overrightarrow{\partial}_\mu + ieA_\mu)\psi - \overline{\psi}\gamma^\mu(\overleftarrow{\partial}_\mu - ieA_\mu)\psi\ ] - m\overline{\psi}\psi - \frac{1}{4}F^{\mu\nu}F_{\mu\nu}\ , \tag{18}$$

and the corresponding energy-momentum tensor is

$$T^{\mu\nu} = \frac{i}{4}\ \Big(\ [\ \overline{\psi}\gamma^\mu(\overrightarrow{\partial}^\nu + ieA^\nu)\psi - \overline{\psi}\gamma^\mu(\overleftarrow{\partial}^\nu - ieA^\nu)\psi\ ]\ +\ [\ \mu \longleftrightarrow \nu\ ]\ \Big)$$

$$+ F^{\mu\rho}F_{\rho}{}^{\nu} + \frac{1}{4}g^{\mu\nu}F^{\rho\lambda}F_{\rho\lambda} \ . \tag{19}$$

Since $T^{\mu\nu}$ is the Noether current of the general coordinate transformation, it is conserved. In later calculations we will identify the two terms in Eq. (19) as the fermion and boson contributions $T^{\mu\nu}_{\rm f}$ and $T^{\mu\nu}_{\rm b}$, respectively.

The physical electron is the eigenstate of the QED Hamiltonian. As discussed in the introduction, the expansion of it is the QED eigenfunction on the complete set $|n\rangle$ of H_0 eigenstates produces the Fock state expansion. It is particularly advantageous to carry out this procedure using light-cone quantization since the vacuum is trivial, the Fock state representation is boost invariant, and the light-cone fractions $x_i = k_i^+/P^+$ are positive: $0 < x_i \leq 1$, $\sum_i x_i = 1$. We also employ light-cone gauge $A^+ = 0$ so that the gauge boson polarizations are physical. Thus each Fock-state wavefunction $\langle n|\text{physical electron}\rangle$ of the physical electron with total spin projection $J^z = \pm\frac{1}{2}$ is represented by the function $\psi_n^{J^z}(x_i, \vec{k}_{\perp i}, \lambda_i)$, where

$$k_i = (k_i^+, k_i^-, \vec{k}_{\perp i}) = \left(x_i P^+, \frac{\vec{k}_{\perp i}^2 + m_i^2}{x_i P^+}, \vec{k}_{\perp i} \right) \tag{20}$$

specifies the momentum of each constituent and λ_i specifies its light-cone helicity in the z direction. We adopt a non-zero boson mass λ for the sake of generality.

The two-particle Fock state for an electron with $J^z = +\frac{1}{2}$ has four possible spin combinations:

$$\begin{aligned} &\left|\Psi^{\uparrow}_{\text{two particle}}(P^+ = 1, \vec{P}_\perp = \vec{0}_\perp)\right\rangle \qquad (21)\\ &= \int \frac{\mathrm{d}^2\vec{k}_\perp \mathrm{d}x}{16\pi^3\sqrt{x(1-x}} \Bigg[\ \psi^{\uparrow}_{+\frac{1}{2}+1}(x, \vec{k}_\perp) \left| +\frac{1}{2} \ +1 \, ; \ x \, , \ \vec{k}_\perp \right\rangle \\ &\quad + \psi^{\uparrow}_{+\frac{1}{2}-1}(x, \vec{k}_\perp) \left| +\frac{1}{2} \ -1 \, ; \ x \, , \ \vec{k}_\perp \right\rangle \\ &\quad + \psi^{\uparrow}_{-\frac{1}{2}+1}(x, \vec{k}_\perp) \left| -\frac{1}{2} \ +1 \, ; \ x \, , \ \vec{k}_\perp \right\rangle \\ &\quad + \psi^{\uparrow}_{-\frac{1}{2}-1}(x, \vec{k}_\perp) \left| -\frac{1}{2} \ -1 \, ; \ x \, , \ \vec{k}_\perp \right\rangle \ \Bigg] \ . \end{aligned}$$

The wavefunctions can be evaluated explicitly in QED perturbation theory using the rules given by Brodsky and Lepage [4] and Brodsky and Drell [31]:

$$\begin{cases} \psi^{\uparrow}_{+\frac{1}{2}+1}(x, \vec{k}_\perp) = -\sqrt{2}\frac{(-k^1 + \mathrm{i}k^2)}{x(1-x)}\,\varphi \ , \\ \psi^{\uparrow}_{+\frac{1}{2}-1}(x, \vec{k}_\perp) = -\sqrt{2}\frac{(+k^1 + \mathrm{i}k^2)}{1-x}\,\varphi \ , \\ \psi^{\uparrow}_{-\frac{1}{2}+1}(x, \vec{k}_\perp) = -\sqrt{2}(M - \frac{m}{x})\,\varphi \ , \\ \psi^{\uparrow}_{-\frac{1}{2}-1}(x, \vec{k}_\perp) = 0 \ , \end{cases} \tag{22}$$

where

$$\varphi = \varphi(x, \vec{k}_\perp) = \frac{e/\sqrt{1-x}}{M^2 - (\vec{k}_\perp^2 + m^2)/x - (\vec{k}_\perp^2 + \lambda^2)/(1-x)} \ . \tag{23}$$

Similarly,

$$\begin{aligned} &\left|\Psi^{\downarrow}_{\text{two particle}}(P^+ = 1, \vec{P}_\perp = \vec{0}_\perp)\right\rangle \\ &= \int \frac{\mathrm{d}^2\vec{k}_\perp \mathrm{d}x}{16\pi^3\sqrt{x(1-x}} \Big[\ \psi^{\downarrow}_{+\frac{1}{2}+1}(x, \vec{k}_\perp) \left|+\frac{1}{2} \ +1 \, ; \ x \, , \ \vec{k}_\perp\right\rangle \\ &\quad + \psi^{\downarrow}_{+\frac{1}{2}-1}(x, \vec{k}_\perp) \left|+\frac{1}{2} \ -1 \, ; \ x \, , \ \vec{k}_\perp\right\rangle \\ &\quad + \psi^{\downarrow}_{-\frac{1}{2}+1}(x, \vec{k}_\perp) \left|-\frac{1}{2} \ +1 \, ; \ x \, , \ \vec{k}_\perp\right\rangle \\ &\quad + \psi^{\downarrow}_{-\frac{1}{2}-1}(x, \vec{k}_\perp) \left|-\frac{1}{2} \ -1 \, ; \ x \, , \ \vec{k}_\perp\right\rangle \ \Big] \ , \end{aligned} \tag{24}$$

where

$$\begin{cases} \psi^{\downarrow}_{+\frac{1}{2}+1}(x, \vec{k}_\perp) = 0 \ , \\ \psi^{\downarrow}_{+\frac{1}{2}-1}(x, \vec{k}_\perp) = -\sqrt{2}(M - \frac{m}{x})\, \varphi \ , \\ \psi^{\downarrow}_{-\frac{1}{2}+1}(x, \vec{k}_\perp) = -\sqrt{2}\frac{(-k^1 + \mathrm{i}k^2)}{1-x}\, \varphi \ , \\ \psi^{\downarrow}_{-\frac{1}{2}-1}(x, \vec{k}_\perp) = -\sqrt{2}\frac{(+k^1 + \mathrm{i}k^2)}{x(1-x)}\, \varphi \ . \end{cases} \tag{25}$$

The coefficients of φ in Eqs. (22) and (25) are the matrix elements of $\frac{\overline{u}(k^+, k^-, \vec{k}_\perp)}{\sqrt{k^+}} \gamma \cdot \epsilon^* \frac{u(P^+, P^-, \vec{P}_\perp)}{\sqrt{P^+}}$ which are the numerators of the wavefunctions corresponding to each constituent spin s^z configuration. The two boson polarization vectors in light-cone gauge are $\epsilon^\mu = (\epsilon^+ = 0 \ , \epsilon^- = \frac{\vec{\epsilon}_\perp \cdot \vec{k}_\perp}{2k^+}, \vec{\epsilon}_\perp)$ where $\vec{\epsilon} = \vec{\epsilon_\perp}_{\uparrow,\downarrow} = \mp(1/\sqrt{2})(\widehat{x} \pm \mathrm{i}\widehat{y})$. The polarizations also satisfy the Lorentz condition $k \cdot \epsilon = 0$.

Note that each Fock state configuration satisfies the spin sum rule: $J^z = S^z_{\mathrm{f}} + s^z_{\mathrm{b}} + l^z = +\frac{1}{2}$. The sign of the helicity of the electron is retained by the leading photon at $x_\gamma = 1 - x \to 1$. Note that in the non-relativistic limit, the transverse motion of the constituents can be neglected, and we have only the $\left|+\frac{1}{2}\right\rangle \to \left|-\frac{1}{2} \ +1\right\rangle$ configuration which is the non-relativistic quantum state for the spin-half system composed of a fermion and a spin-1 boson constituents. The fermion constituent has spin projection in the opposite direction to the spin J^z of the whole system. However, for ultra-relativistic binding in which the transversal motions of the constituents are large compared to the fermion masses, the $\left|+\frac{1}{2}\right\rangle \to \left|+\frac{1}{2} \ +1\right\rangle$ and $\left|+\frac{1}{2}\right\rangle \to \left|+\frac{1}{2} \ -1\right\rangle$ configurations dominate over the $\left|+\frac{1}{2}\right\rangle \to \left|-\frac{1}{2} \ +1\right\rangle$ configuration. In this case the fermion constituent has spin projection parallel to J^z.

We can see how the angular momentum sum rule is satisfied for the wavefunctions Eqs. (21) and (24) of the QED model system. In Table 1 we list the fermion

constituent's light-cone spin projection $s^z_{\rm f} = \frac{1}{2}\lambda_{\rm f}$, the boson constituent spin projection $s^z_{\rm b} = \lambda_{\rm b}$, and the relative orbital angular momentum l^z for each contributing configuration of the QED model system wavefunction. Table 1 is derived by calculat-

Table 1. Spin Decomposition of the $J^z_e = +1/2$ Electron

Configuration	Fermion Spin $s^z_{\rm f}$	Boson Spin $s^z_{\rm b}$	Orbital Ang. Mom. l^z
$\vert{+\frac{1}{2}}\rangle \to \vert{+\frac{1}{2}}\ {+1}\rangle$	$+\frac{1}{2}$	$+1$	-1
$\vert{+\frac{1}{2}}\rangle \to \vert{-\frac{1}{2}}\ {+1}\rangle$	$-\frac{1}{2}$	$+1$	0
$\vert{+\frac{1}{2}}\rangle \to \vert{+\frac{1}{2}}\ {-1}\rangle$	$+\frac{1}{2}$	-1	$+1$

ing the matrix elements of the light-cone helicity operator $\gamma^+\gamma^5$ [43] and the relative orbital angular momentum operator $-{\rm i}(k^1\frac{\partial}{\partial k^2} - k^2\frac{\partial}{\partial k^1})$ [37, 44, 45] in the light-cone representation. Each configuration satisfies the spin sum rule: $J^z = s^z_{\rm f} + s^z_{\rm b} + l^z$.

The electron in QED also has a "bare" one-particle component:

$$|\Psi^{\uparrow,\downarrow}_{\text{one particle}}\rangle = \sqrt{Z}\ \delta(1-x)\ \delta(\vec{k}_\perp = \vec{0}_\perp)\ \delta_{s^z_{\rm f}\ \pm\frac{1}{2}}\ , \tag{26}$$

where Z is the wavefunction normalization of the one-particle state. If we regulate the theory in the ultraviolet and infrared, Z is finite.

We first will evaluate the Dirac and Pauli form factors $F_1(q^2)$ and $F_2(q^2)$. Using Eqs. (6) and (21) we have to order e^2

$$\begin{aligned} F_1(q^2) &= \Big\langle \Psi^\uparrow(p^+ = 1, \vec{P}_\perp = \vec{q}_\perp))|\Psi^\uparrow(p^+ = 1, \vec{P}_\perp = \vec{0}_\perp)\Big\rangle \\ &= Z + \int \frac{{\rm d}^2\vec{k}_\perp {\rm d}x}{16\pi^3}\Big[\psi^{\uparrow\ *}_{+\frac{1}{2}+1}(x,\vec{k}'_\perp)\psi^\uparrow_{+\frac{1}{2}+1}(x,\vec{k}_\perp) \\ &\quad +\psi^{\uparrow\ *}_{+\frac{1}{2}-1}(x,\vec{k}'_\perp)\psi^\uparrow_{+\frac{1}{2}-1}(x,\vec{k}_\perp) + \psi^{\uparrow\ *}_{-\frac{1}{2}+1}(x,\vec{k}'_\perp)\psi^\uparrow_{-\frac{1}{2}+1}(x,\vec{k}_\perp)\Big]\ , \end{aligned} \tag{27}$$

where

$$\vec{k}'_\perp = \vec{k}_\perp + (1-x)\vec{q}_\perp\ . \tag{28}$$

Ultraviolet regularization is assumed. For example, we can assume a cutoff in the invariant mass of the constituents: $\mathcal{M}^2 = \sum_i \frac{\vec{k}^2_{\perp i} + m^2_i}{x_i} < \Lambda^2$.

At zero momentum transfer

$$\begin{aligned} F_1(0) &= Z + \int \frac{{\rm d}^2\vec{k}_\perp {\rm d}x}{16\pi^3}\Big[\psi^{\uparrow\ *}_{+\frac{1}{2}+1}(x,\vec{k}_\perp)\psi^\uparrow_{+\frac{1}{2}+1}(x,\vec{k}_\perp) \\ &\quad +\psi^{\uparrow\ *}_{+\frac{1}{2}-1}(x,\vec{k}_\perp)\psi^\uparrow_{+\frac{1}{2}-1}(x,\vec{k}_\perp) + \psi^{\uparrow\ *}_{-\frac{1}{2}+1}(x,\vec{k}_\perp)\psi^\uparrow_{-\frac{1}{2}+1}(x,\vec{k}_\perp)\Big]\ . \end{aligned} \tag{29}$$

We can simulate a composite model of two particles by choosing the coupling strength $e(\Lambda)$ such that $F_1(0) = 1$ is satisfied. The one-loop model can be further generalized by applying spectral Pauli-Villars integration over the constituent masses. The resulting form of light-cone wavefunctions provides a template for parameterizing the structure of relativistic composite systems and their matrix elements in hadronic physics.

The Pauli form factor is obtained from the spin-flip matrix element of the J^+ current. From Eqs. (7), (21), and (24) we have

$$\begin{aligned}
F_2(q^2) &= \frac{-2M}{(q^1 - \mathrm{i}q^2)} \left\langle \Psi^{\uparrow}(P^+ = 1, \vec{P}_\perp = \vec{q}_\perp)) | \Psi^{\downarrow}(P^+ = 1, \vec{P}_\perp = \vec{0}_\perp) \right\rangle \\
&= \frac{-2M}{(q^1 - \mathrm{i}q^2)} \int \frac{\mathrm{d}^2\vec{k}_\perp \mathrm{d}x}{16\pi^3} \Big[\psi^{\uparrow\,*}_{+\frac{1}{2}\,-1}(x, \vec{k}'_\perp) \psi^{\downarrow}_{+\frac{1}{2}\,-1}(x, \vec{k}_\perp) \\
&\quad + \psi^{\uparrow\,*}_{-\frac{1}{2}\,+1}(x, \vec{k}'_\perp) \psi^{\downarrow}_{-\frac{1}{2}\,+1}(x, \vec{k}_\perp) \Big] \\
&= 4M \int \frac{\mathrm{d}^2\vec{k}_\perp \mathrm{d}x}{16\pi^3} \frac{(m - Mx)}{x} \varphi(x, \vec{k}'_\perp)^* \varphi(x, \vec{k}_\perp) \\
&= 4Me^2 \int \frac{\mathrm{d}^2\vec{k}_\perp \mathrm{d}x}{16\pi^3} \frac{(m - xM)}{x(1-x)} \\
&\quad \times \frac{1}{\left[M^2 - \frac{(\vec{k}_\perp + (1-x)\vec{q}_\perp)^2 + m^2}{x} - \frac{(\vec{k}_\perp + (1-x)\vec{q}_\perp)^2 + \lambda^2}{1-x} \right]} \\
&\quad \times \frac{1}{\left[M^2 - \frac{\vec{k}_\perp^2 + m^2}{x} - \frac{\vec{k}_\perp^2 + \lambda^2}{1-x} \right]} \,. \qquad (30)
\end{aligned}$$

Using the Feynman parameterization, we can also express Eq. (30) in a form in which the $q^2 = -\vec{q}_\perp^2$ dependence is more explicit as

$$F_2(q^2) = \frac{Me^2}{4\pi^2} \int_0^1 d\alpha \int_0^1 dx \, \frac{m - xM}{\alpha(1-\alpha)\frac{1-x}{x}\vec{q}_\perp^2 - M^2 + \frac{m^2}{x} + \frac{\lambda^2}{1-x}} \,. \qquad (31)$$

The anomalous moment is obtained in the limit of zero momentum transfer:

$$\begin{aligned}
F_2(0) &= 4Me^2 \int \frac{\mathrm{d}^2\vec{k}_\perp \mathrm{d}x}{16\pi^3} \frac{(m - xM)}{x(1-x)} \frac{1}{\left[M^2 - \frac{\vec{k}_\perp^2 + m^2}{x} - \frac{\vec{k}_\perp^2 + \lambda^2}{1-x} \right]^2} \\
&= \frac{Me^2}{4\pi^2} \int_0^1 dx \, \frac{m - xM}{-M^2 + \frac{m^2}{x} + \frac{\lambda^2}{1-x}} \,, \qquad (32)
\end{aligned}$$

which is the result of Brodsky and Drell.[31] For zero photon mass and $M = m$, it gives the correct order α Schwinger value $a_e = F_2(0) = \alpha/2\pi$ for the electron anomalous magnetic moment for QED.

As seen from Eqs. (14) and (15), the matrix elements of the double plus components of the energy-momentum tensor are sufficient to derive the fermion and boson constituents' form factors $A_{\rm f,g}(q^2)$ and $B_{\rm f,g}(q^2)$ of graviton coupling to matter. In particular, we shall verify $A(0) = A_{\rm f}(0) + A_{\rm b}(0) = 1$ and $B(0) = 0$.

The individual contributions of the fermion and boson fields to the energy-momentum form factors in QED are given by

$$\begin{aligned} A_{\rm f}(q^2) &= \left\langle \Psi^{\uparrow}(P^+ = 1, \vec{P}_\perp = \vec{q}_\perp) \right| \frac{T_{\rm f}^{++}(0)}{2(P^+)^2} \left| \Psi^{\uparrow}(P^+ = 1, \vec{P}_\perp = \vec{0}_\perp) \right\rangle \\ &= \int \frac{{\rm d}^2\vec{k}_\perp {\rm d}x}{16\pi^3}\, x \left[\psi^{\uparrow\,*}_{+\frac{1}{2}+1}(x, \vec{k}'_\perp) \psi^{\uparrow}_{+\frac{1}{2}+1}(x, \vec{k}_\perp) \right. \\ &\quad \left. + \psi^{\uparrow\,*}_{+\frac{1}{2}-1}(x, \vec{k}'_\perp) \psi^{\uparrow}_{+\frac{1}{2}-1}(x, \vec{k}_\perp) + \psi^{\uparrow\,*}_{-\frac{1}{2}+1}(x, \vec{k}'_\perp) \psi^{\uparrow}_{-\frac{1}{2}+1}(x, \vec{k}_\perp) \right] , \end{aligned} \tag{33}$$

where $\vec{k}'_\perp$ is given in Eq. (28), and

$$\begin{aligned} A_{\rm b}(q^2) &= \left\langle \Psi^{\uparrow}(P^+ = 1, \vec{P}_\perp = \vec{q}_\perp) \right| \frac{T_{\rm b}^{++}(0)}{2(P^+)^2} \left| \Psi^{\uparrow}(P^+ = 1, \vec{P}_\perp = \vec{0}_\perp) \right\rangle \\ &= \int \frac{{\rm d}^2\vec{k}_\perp {\rm d}x}{16\pi^3}\, (1-x) \left[\psi^{\uparrow\,*}_{+\frac{1}{2}+1}(x, \vec{k}''_\perp) \psi^{\uparrow}_{+\frac{1}{2}+1}(x, \vec{k}_\perp) \right. \\ &\quad \left. + \psi^{\uparrow\,*}_{+\frac{1}{2}-1}(x, \vec{k}''_\perp) \psi^{\uparrow}_{+\frac{1}{2}-1}(x, \vec{k}_\perp) + \psi^{\uparrow\,*}_{-\frac{1}{2}+1}(x, \vec{k}''_\perp) \psi^{\uparrow}_{-\frac{1}{2}+1}(x, \vec{k}_\perp) \right] , \end{aligned} \tag{34}$$

where

$$\vec{k}''_\perp = \vec{k}_\perp - x\vec{q}_\perp \ . \tag{35}$$

Note that

$$A_{\rm f}(0) + A_{\rm b}(0) = F_1(0) = 1 \ , \tag{36}$$

which corresponds to the momentum sum rule.

The fermion and boson contributions to the spin-flip matter form factor are

$$\begin{aligned} B_{\rm f}(q^2) &= \frac{-2M}{(q^1 - {\rm i}q^2)} \left\langle \Psi^{\uparrow}(P^+ = 1, \vec{P}_\perp = \vec{q}_\perp) \right| \frac{T_{\rm f}^{++}(0)}{2(P^+)^2} \left| \Psi^{\downarrow}(P^+ = 1, \vec{P}_\perp = \vec{0}_\perp) \right\rangle \\ &= \frac{-2M}{(q^1 - {\rm i}q^2)} \int \frac{{\rm d}^2\vec{k}_\perp {\rm d}x}{16\pi^3}\, x \left[\psi^{\uparrow\,*}_{+\frac{1}{2}-1}(x, \vec{k}'_\perp) \psi^{\downarrow}_{+\frac{1}{2}-1}(x, \vec{k}_\perp) \right. \\ &\quad \left. + \psi^{\uparrow\,*}_{-\frac{1}{2}+1}(x, \vec{k}'_\perp) \psi^{\downarrow}_{-\frac{1}{2}+1}(x, \vec{k}_\perp) \right] \\ &= 4M \int \frac{{\rm d}^2\vec{k}_\perp {\rm d}x}{16\pi^3} (m - Mx) \varphi(x, \vec{k}'_\perp)^* \varphi(x, \vec{k}_\perp) \\ &= 4Me^2 \int \frac{{\rm d}^2\vec{k}_\perp {\rm d}x}{16\pi^3} \frac{(m - xM)}{(1-x)} \\ &\quad \times \frac{1}{\left[M^2 - \frac{(\vec{k}_\perp + (1-x)\vec{q}_\perp)^2 + m^2}{x} - \frac{(\vec{k}_\perp + (1-x)\vec{q}_\perp)^2 + \lambda^2}{1-x} \right]} \end{aligned}$$

$$\times \frac{1}{\left[M^2 - \frac{\vec{k}_\perp^2+m^2}{x} - \frac{\vec{k}_\perp^2+\lambda^2}{1-x}\right]}$$

$$= \frac{Me^2}{4\pi^2}\int_0^1 d\alpha \int_0^1 dx \, \frac{x(m-xM)}{\alpha(1-\alpha)\,\frac{1-x}{x}\,\vec{q}_\perp^2 - M^2 + \frac{m^2}{x} + \frac{\lambda^2}{1-x}} \,, \tag{37}$$

and

$$\begin{aligned}
B_{\rm b}(q^2) &= \frac{-2M}{(q^1-{\rm i}q^2)}\left\langle \Psi^\uparrow(P^+=1,\vec{P}_\perp=\vec{q}_\perp)\right| \frac{T_{\rm b}^{++}(0)}{2(P^+)^2}\left|\Psi^\downarrow(P^+=1,\vec{P}_\perp=\vec{0}_\perp)\right\rangle \\
&= \frac{-2M}{(q^1-{\rm i}q^2)}\int \frac{{\rm d}^2\vec{k}_\perp {\rm d}x}{16\pi^3}\,(1-x) \\
&\qquad \times\left[\psi^{\uparrow\,*}_{+\frac{1}{2}\,-1}(x,\vec{k}'_\perp)\psi^\downarrow_{+\frac{1}{2}\,-1}(x,\vec{k}_\perp) + \psi^{\uparrow\,*}_{-\frac{1}{2}\,+1}(x,\vec{k}'_\perp)\psi^\downarrow_{-\frac{1}{2}\,+1}(x,\vec{k}_\perp)\right] \\
&= -4M\int \frac{{\rm d}^2\vec{k}_\perp {\rm d}x}{16\pi^3}(m-Mx)\varphi(x,\vec{k}'_\perp)^*\varphi(x,\vec{k}_\perp) \\
&= -4Me^2\int \frac{{\rm d}^2\vec{k}_\perp {\rm d}x}{16\pi^3}\frac{(m-xM)}{(1-x)} \\
&\quad \times\frac{1}{[M^2-((\vec{k}_\perp-x\vec{q}_\perp)^2+m^2)/x-((\vec{k}_\perp-x\vec{q}_\perp)^2+\lambda^2)/(1-x)]} \\
&\quad \times\frac{1}{[M^2-(\vec{k}_\perp^2+m^2)/x-(\vec{k}_\perp^2+\lambda^2)/(1-x)]} \\
&= -\frac{Me^2}{4\pi^2}\int_0^1 d\alpha \int_0^1 dx \, \frac{x(m-xM)}{\alpha(1-\alpha)\,\frac{x}{1-x}\,\vec{q}_\perp^2 - M^2 + \frac{m^2}{x} + \frac{\lambda^2}{1-x}} \,.
\end{aligned} \tag{38}$$

The total contribution for general momentum transfer is

$$\begin{aligned}
&B(q^2) = B_{\rm f}(q^2) + B_{\rm b}(q^2) \\
&= 4Me^2\int \frac{{\rm d}^2\vec{k}_\perp {\rm d}x}{16\pi^3}\frac{(m-xM)}{(1-x)} \\
&\quad \times\{\frac{1}{[M^2-((\vec{k}_\perp+(1-x)\vec{q}_\perp)^2+m^2)/x-((\vec{k}_\perp+(1-x)\vec{q}_\perp)^2+\lambda^2)/(1-x)]} \\
&\qquad -\frac{1}{[M^2-((\vec{k}_\perp-x\vec{q}_\perp)^2+m^2)/x-((\vec{k}_\perp-x\vec{q}_\perp)^2+\lambda^2)/(1-x)]}\} \\
&\quad \times\frac{1}{[M^2-(\vec{k}_\perp^2+m^2)/x-(\vec{k}_\perp^2+\lambda^2)/(1-x)]} \\
&= \frac{Me^2}{4\pi^2}\int_0^1 d\alpha \int_0^1 dx \; x(m-xM) \\
&\quad \times\Big(\frac{1}{\alpha(1-\alpha)\,\frac{1-x}{x}\,\vec{q}_\perp^2 - M^2 + \frac{m^2}{x} + \frac{\lambda^2}{1-x}} - \frac{1}{\alpha(1-\alpha)\,\frac{x}{1-x}\,\vec{q}_\perp^2 - M^2 + \frac{m^2}{x} + \frac{\lambda^2}{1-x}}\Big) \,.
\end{aligned} \tag{39}$$

This is the analog of the Pauli form factor for a physical electron scattering in a gravitational field and in general is not zero. However at zero momentum transfer

$$B(0) = B_{\rm f}(0) + B_{\rm b}(0) = 0. \tag{40}$$

This result agree with the conclusions of Okun and Kobzarev [38], Ji [35] and Teryaev.[42]

The helicity-flip electromagnetic and gravitational form factors for the fluctuations of the electron at one-loop are illustrated in Fig. 1. The cancelation of the sum of graviton couplings $B(q^2)$ to the constituents at $q^2 = 0$ is evident.

5 The Anomalous Gravitomagnetic Moment for Composite Systems

A remarkable property of gravitational interactions is that the anomalous gravitomagnetic moment $B(0) = 0$ vanishes identically for each contributing Fock state of a composite system.[8] In order to calculate $B(0)$ by using Eq. (15), we need to consider a non-forward amplitude. The internal momentum variables for the final state wavefunction are given by Eqs. (11) and (12). The subscripts of x_i and $\vec{k}_{\perp i}$ label constituent particles, the superscripts of $q^1_\perp$, $k^1_\perp$, and $k^2_\perp$ label the Lorentz indices, and the subscript a in ψ_a indicates the contributing Fock state. The essential ingredient is the Lorentz property of the light-cone wavefunctions.

It is important to identify the $n-1$ independent relative momenta of the n-particle Fock state.

$$\begin{aligned}
-\frac{B(0)}{2M} &= \lim_{q^1_\perp \to 0} \frac{\partial}{\partial q^1_\perp} \left\langle P+q, \uparrow \left| \frac{T^{++}(0)}{2(P^+)^2} \right| P, \downarrow \right\rangle \qquad (41)\\
&= \lim_{q^1_\perp \to 0} \frac{\partial}{\partial q^1_\perp} \left\langle \Psi^\uparrow(P^+ = 1, \vec{P}_\perp = \vec{q}_\perp)) \left| \frac{T^{++}(0)}{2(P^+)^2} \right| \Psi^\downarrow(P^+ = 1, \vec{P}_\perp = \vec{0}_\perp) \right\rangle \\
&= \lim_{q^1_\perp \to 0} \frac{\partial}{\partial q^1_\perp} \sum_a \int \prod_{k=1}^{n-1} \frac{{\rm d}^2 \vec{k}_{\perp k} {\rm d}x_k}{16\pi^3} \\
&\times \psi_a^{\uparrow *}\Big(x_1, x_2, \cdots, x_{n-1}, (1 - x_1 - x_2 - \cdots - x_{n-1}), \\
&\qquad \vec{k}'_{\perp 1}, \vec{k}'_{\perp 2}, \cdots, \vec{k}'_{\perp n-1}, (-\vec{k}'_{\perp 1} - \vec{k}'_{\perp 2} - \cdots - \vec{k}'_{\perp n-1})\Big) \\
&\times \Big[\sum_{i=1}^{n-1} x_i + (1 - x_1 - x_2 - \cdots - x_{n-1})\Big] \\
&\times \psi_a^{\downarrow}\Big(x_1, x_2, \cdots, x_{n-1}, (1 - x_1 - x_2 - \cdots - x_{n-1}), \\
&\qquad \vec{k}_{\perp 1}, \vec{k}_{\perp 2}, \cdots, \vec{k}_{\perp n-1}, (-\vec{k}_{\perp 1} - \vec{k}_{\perp 2} - \cdots - \vec{k}_{\perp n-1})\Big) \ .
\end{aligned}$$

Using integration by parts,

$$-\frac{B_a(0)}{2M} = \qquad (42)$$

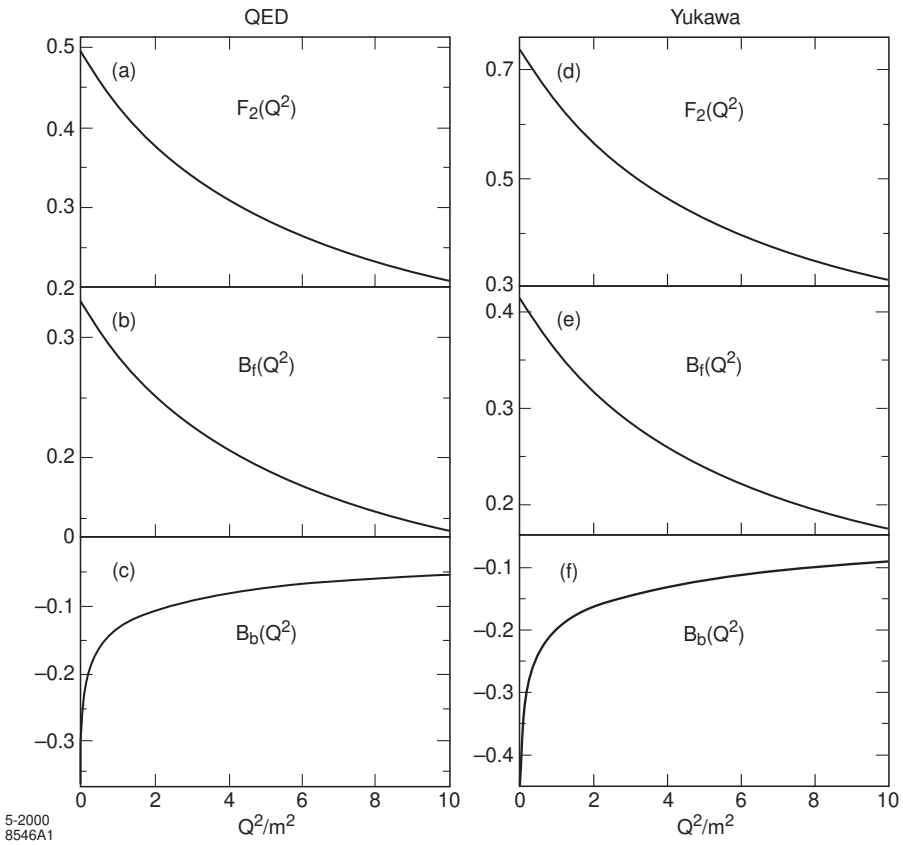

Figure 1: Helicity-flip electromagnetic and gravitational form factors for space-like $q^2 = -Q^2 < 0$ from the quantum fluctuations of a fermion at one-loop order in units of α/π for QED and $g^2/4\pi^2$ for the Yukawa theory. The fermion constituent mass is taken as $m_f = M$. The boson constituent is massless. (a) Helicity-flip Pauli form factor $F_2(q^2)$ in QED. Notice that $F_2(0) = 1/2$. (b) Helicity-flip form factor $B_b(q^2)$ of the graviton coupling to the boson (photon) constituent of the electron at one-loop order in QED. Notice that $B_b(0) = -1/3$. (c) Helicity-flip fermion form factor $B_f(q^2)$ of the graviton coupling to the fermion constituent at one-loop order in QED. Notice that $B_f(0) = 1/3$, and thus $B_f(0) + B_b(0) = 0$. (d) Helicity-flip Pauli form factor $F_2(q^2)$ in the Yukawa theory. Notice that in this case $F_2(0) = 3/4$. (e) Helicity-flip form factor $B_b(q^2)$ of the graviton coupling to the boson at one-loop order in the Yukawa theory. Notice that $B_b(0) = -5/12$. (f) Helicity-flip fermion form factor $B_f(q^2)$ of the graviton coupling to the fermion constituent at one-loop order in the Yukawa theory. Notice that $B_f(0) = 5/12$, and thus $B_f(0) + B_b(0) = 0$.

$$
\begin{aligned}
&= \int \prod_{k=1}^{n-1} \frac{\mathrm{d}^2\vec{k}_{\perp k}\mathrm{d}x_k}{16\pi^3} \psi_a^{\uparrow *}\Big(x_1, x_2, \cdots, x_{n-1}, (1 - x_1 - x_2 - \cdots - x_{n-1}), \\
&\qquad \vec{k}_{\perp 1}, \vec{k}_{\perp 2}, \cdots, \vec{k}_{\perp n-1}, (-\vec{k}_{\perp 1} - \vec{k}_{\perp 2} - \cdots - \vec{k}_{\perp n-1})\Big) \\
&\times \Big[\sum_{i=1}^{n-1} x_i \Big((-1 + x_i) \frac{\partial}{\partial k^1_{\perp i}} + \sum_{j \neq i}^{n-1} x_j \frac{\partial}{\partial k^1_{\perp j}} \Big) \\
&\qquad + (1 - x_1 - x_2 - \cdots - x_{n-1}) \sum_{j=1}^{n-1} x_j \frac{\partial}{\partial k^1_{\perp j}} \Big] \\
&\times \psi_a^{\downarrow}\Big(x_1, x_2, \cdots, x_{n-1}, (1 - x_1 - x_2 - \cdots - x_{n-1}), \\
&\qquad \vec{k}_{\perp 1}, \vec{k}_{\perp 2}, \cdots, \vec{k}_{\perp n-1}, (-\vec{k}_{\perp 1} - \vec{k}_{\perp 2} - \cdots - \vec{k}_{\perp n-1})\Big) \\
&= \int \prod_{k=1}^{n-1} \frac{\mathrm{d}^2\vec{k}_{\perp k}\mathrm{d}x_k}{16\pi^3} \psi_a^{\uparrow *}\Big(x_1, x_2, \cdots, x_{n-1}, (1 - x_1 - x_2 - \cdots - x_{n-1}), \\
&\qquad \vec{k}_{\perp 1}, \vec{k}_{\perp 2}, \cdots, \vec{k}_{\perp n-1}, (-\vec{k}_{\perp 1} - \vec{k}_{\perp 2} - \cdots - \vec{k}_{\perp n-1})\Big) \\
&\times \Big[\sum_{i=1}^{n-1} \Big(-1 + \sum_{j=1}^{n-1} x_j + (1 - x_1 - x_2 - \cdots - x_{n-1}) \Big) x_i \frac{\partial}{\partial k^1_{\perp i}} \Big] \\
&\times \psi_a^{\downarrow}\Big(x_1, x_2, \cdots, x_{n-1}, (1 - x_1 - x_2 - \cdots - x_{n-1}), \\
&\qquad \vec{k}_{\perp 1}, \vec{k}_{\perp 2}, \cdots, \vec{k}_{\perp n-1}, (-\vec{k}_{\perp 1} - \vec{k}_{\perp 2} - \cdots - \vec{k}_{\perp n-1})\Big) \\
&= 0 \ .
\end{aligned}
$$

Thus the contribution $B_a(0)$ to the total anomalous gravitomagnetic moment $B(0)$ vanishes separately from each contributing Fock state a.

6 The Perturbative Model as a Template for a Composite System

The spin structure of perturbative theory provides a template for the numerator structure of the light-cone wavefunctions even for composite systems since the equations which couple different Fock components mimic the perturbative form. For example, the structure of the electron's Fock state in perturbative QED shows that it is natural to have a negative contribution from relative orbital angular momentum which balances the S_z of its photon constituents. We can thus expect a large orbital contribution to the proton's J_z since gluons carry roughly half of the proton's momentum, thus providing insight into the "spin crisis" in QCD.

We can generalize the perturbative model by using the structure of the one-loop QED (and Yukawa) calculations with general values for general values of the external mass M, internal fermion mass m, and boson mass λ, to represent a spin-$\frac{1}{2}$ system composed of a fermion and a spin-1 or spin-0 boson. Such a model describes an effec-

tively composite system with no bare one-particle Fock state. We can also generalize the functional form of the momentum space wavefunction $\varphi(x, \vec{k}_\perp)$ by introducing a spectrum of vector bosons satisfying the generalized Pauli-Villars spectral conditions

$$\int d\lambda^2 \lambda^{2N} \rho(\lambda^2) = 0, \quad N = 0, 1, \cdots . \tag{43}$$

For example, we can simulate a proton as a bound state of a quark and diquark [46], using spin-0, spin-1 diquarks, or a linear superposition of the two states. The model can be made to match the power-law fall-off of the hadron form factors predicted in perturbative QCD by the choice of sum rule conditions on the Pauli-Villars spectra.[47, 48] The light-cone framework of the model resembles that of the covariant parton model of Landshoff, Polkinghorne and Short [49, 50], in which the power behavior of the spectral integral at high masses corresponds to the Regge behavior of the deep inelastic structure functions. Although the model is based on just two Fock constituents, it is relativistic and satisfies self-consistency conditions such as in the point-like limit where $R^2 M^2 \to 0$, the anomalous moment vanishes.[34] The light-cone formalism also properly incorporates Wigner boosts. Thus this model of composite systems can serve as a useful theoretical laboratory to interrelate hadronic properties and check the consistency of formulae proposed for the study of hadron substructure.

In the case of Yukawa theory at one loop, the non-relativistic fermion's spin projection is aligned with the total J^z, and it is anti-aligned in the ultra-relativistic limit. The distinct features of spin structure in the non-relativistic and ultra-relativistic limits reveals the importance of relativistic effects and supports the viewpoint [43, 51, 52] that the proton "spin puzzle" can be understood as due to the relativistic motion of quarks inside the nucleon. In particular, the spin projection of the relativistic constituent quark tends to be anti-aligned with the proton spin in a quark-diquark bound state if the diquark has spin 0. The state with orbital angular momentum $l^z = \pm 1$ in fact dominates over the states with $l^z = 0$. Thus the empirical fact that Δq is small in the proton has a natural description in the light-cone Fock representation of hadrons.

7 Light-cone Representation of Deeply Virtual Compton Scattering

The virtual Compton scattering process $\frac{d\sigma}{dt}(\gamma^* p \to \gamma p)$ for large initial photon virtuality $q^2 = -Q^2$ (see Fig. 2) has extraordinary sensitivity to fundamental features of the proton's structure. Even though the final state photon is on-shell, the deeply virtual process probes the elementary quark structure of the proton near the light cone as an effective local current. In contrast to deep inelastic scattering, which measures only the absorptive part of the forward virtual Compton amplitude $Im\mathcal{T}_{\gamma^* p \to \gamma^* p}$, deeply virtual Compton scattering allows the measurement of the phase and spin structure of proton matrix elements for general momentum transfer squared t. In addition, the

interference of the virtual Compton amplitude and Bethe-Heitler wide angle scattering Bremsstrahlung amplitude where the photon is emitted from the lepton line leads to an electron-positron asymmetry in the $e^{\pm}p \to e^{\pm}\gamma p$ cross section which is proportional to the real part of the Compton amplitude.[53] The deeply virtual Compton amplitude $\gamma^* p \to \gamma p$ is related by crossing to another important process $\gamma^*\gamma \to$ hadron pairs at fixed invariant mass which can be measured in electron-photon collisions.[54]

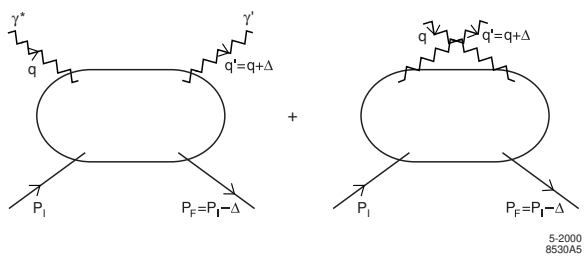

Figure 2: The virtual Compton amplitude $\gamma^*(q)p_I \to \gamma(q')p_F$.

To leading order in $1/Q$, the deeply virtual Compton scattering amplitude factorizes as the convolution in x of the amplitude $t^{\mu\nu}$ for hard Compton scattering on a quark line with the generalized Compton form factors $H(x,t,\zeta)$, $E(x,t,\zeta)$, $\tilde{H}(x,t,\zeta)$, and $\tilde{E}(x,t,\zeta)$ of the target proton.[55, 56, 57, 58] [59, 60, 61, 62, 63, 64, 65] Here x is the light-cone momentum fraction of the struck quark, and $\zeta = Q^2/2P\cdot q$ plays the role of the Bjorken variable. The square of the four-momentum transfer from the proton is given by

$$t = \Delta^2 \;=\; 2P\cdot\Delta \;=\; -\frac{(\zeta^2 M^2 + \vec{\Delta}_\perp^2)}{(1-\zeta)} \;, \tag{44}$$

where Δ is the difference of initial and final momenta of the proton ($P = P' + \Delta$). The form factor $H(x,t,\zeta)$ describes the proton response when the helicity of the proton is unchanged, and $E(x,t,\zeta)$ is for the case when the proton helicity is flipped. Two additional functions $\tilde{H}(x,t,\zeta)$, and $\tilde{E}(x,t,\zeta)$ appear, corresponding to the dependence of the Compton amplitude on quark helicity.

The kinematics of virtual Compton scattering $\gamma^*(q)p(P) \to \gamma(q')p(P')$ are illustrated in Fig. 3. We specify the frame by choosing a convenient parameterization of the light-cone coordinates for the initial and final proton:

$$P_I = (P^+ \;,\; \vec{P}_\perp \;,\; P^-) \;=\; \left(P^+ \;,\; \vec{0}_\perp \;,\; \frac{M^2}{P^+} \right) \;, \tag{45}$$

$$P_F = (P'^+ \;,\; \vec{P}'_\perp \;,\; P'^-) \;=\; \left((1-\zeta)P^+ \;,\; -\vec{\Delta}_\perp \;,\; \frac{(M^2 + \vec{\Delta}_\perp^2)}{(1-\zeta)P^+} \right) \;. \tag{46}$$

(Our metric is specified by $V^{\pm} = V^0 \pm V^z$ and $V^2 = V^+V^- - V_\perp^2$.) The four-momentum transfer from the target is

$$\Delta = P_I - P_F \;=\; (\Delta^+ \;,\; \vec{\Delta}_\perp \;,\; \Delta^-) \;=\; \left(\zeta P^+ \;,\; \vec{\Delta}_\perp \;,\; \frac{(t + \vec{\Delta}_\perp^2)}{\zeta P^+}\right) \;,$$

where $\Delta^2 = t$. In addition, overall energy-momentum conservation requires $\Delta^- = P_I^I - P_F^-$.

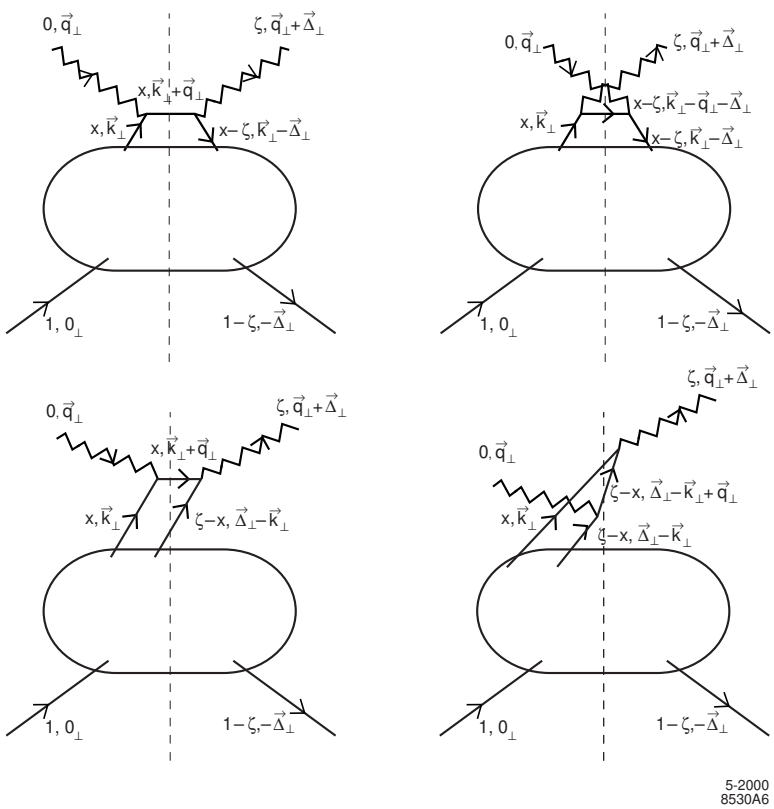

Figure 3: Light-cone time-ordered contributions to deeply virtual Compton scattering. Only the contributions of leading twist in $1/q^2$ are illustrated. These contributions illustrate the factorization property of the leading twist amplitude.

As in the case of space-like form factors, it is convenient to choose a frame where the incident space-like photon carries $q^+ = 0$ and $q^2 = -Q^2 = -\vec{q}_\perp^2$:

$$q = (q^+ \;,\; \vec{q}_\perp \;,\; q^-) \;=\; \left(0 \;,\; \vec{q}_\perp \;,\; \frac{(\vec{q}_\perp + \vec{\Delta}_\perp)^2}{\zeta P^+} + \frac{(\zeta M^2 + \vec{\Delta}_\perp^2)}{(1-\zeta)P^+}\right) \;, \tag{47}$$

$$q' = (q'^+ \ , \ \vec{q}'_\perp \ , \ q'^-) \ = \ \left(\zeta P^+ \ , \ (\vec{q}_\perp + \vec{\Delta}_\perp) \ , \ \frac{(\vec{q}_\perp + \vec{\Delta}_\perp)^2}{\zeta P^+} \right) \ = q + \Delta. \tag{48}$$

Thus no light-cone time-ordered amplitudes involving the splitting of the incident photon can occur. The connection between $\vec{\Delta}_\perp^2$, ζ, and t is given by Eq. (44). The variable ζ is fixed from (45) and (48)

$$2P_I \cdot q = \frac{(\vec{q}_\perp + \vec{\Delta}_\perp)^2}{\zeta} + \frac{(\zeta M^2 + \vec{\Delta}_\perp^2)}{(1-\zeta)} \ . \tag{49}$$

We will be interested in deeply virtual Compton scattering where q^2 is large compared to the masses and t. Then, to leading order in $1/Q^2$, we can take

$$\frac{-q^2}{2P_I \cdot q} = \zeta \ . \tag{50}$$

Thus ζ plays the role of the Bjorken variable in deeply virtual Compton scattering. For a fixed value of $-t$, the allowed range of ζ is given by

$$0 \ \leq \ \zeta \ \leq \ \frac{(-t)}{2M^2} \ \left(\sqrt{1 + \frac{4M^2}{(-t)}} \ - \ 1 \right) \ . \tag{51}$$

The choice of parameterization of the light-cone frame is of course arbitrary. For example, one can also conveniently utilize a "symmetric" frame for the ingoing and outgoing proton which has manifest $\Delta \to -\Delta$ symmetry.

Recently, Markus Diehl, Dae Sung Hwang and I [30] have shown how the deeply virtual Compton amplitude can be evaluated explicitly in the Fock state representation using the matrix elements of the currents and the boost properties of the light-cone wavefunctions. For the $n \to n$ diagonal term ($\Delta n = 0$), the arguments of the final-state hadron wavefunction are $\frac{x_1 - \zeta}{1-\zeta}$, $\vec{k}_{\perp 1} - \frac{1-x_1}{1-\zeta}\vec{\Delta}_\perp$ for the struck quark and $\frac{x_i}{1-\zeta}$, $\vec{k}_{\perp i} + \frac{x_i}{1-\zeta}\vec{\Delta}_\perp$ for the $n-1$ spectators. We thus obtain formulae for the diagonal (parton-number-conserving) contribution to the generalized form factors for deeply virtual Compton amplitude in the domain[63, 64, 66] $\zeta \leq x_1 \leq 1$:

$$\begin{aligned} &\sqrt{1-\zeta} f_{1\,(n\to n)}(x_1, t, \zeta) \ - \ \frac{\zeta^2}{4\sqrt{1-\zeta}} f_{2\,(n\to n)}(x_1, t, \zeta) \\ &= \sum_{n,\ \lambda} \prod_{i=1}^{n} \int_0^1 dx_{i(i\neq 1)} \int \frac{d^2\vec{k}_{\perp i}}{2(2\pi)^3} \ \delta \left(1 - \sum_{j=1}^{n} x_j \right) \ \delta^{(2)} \left(\sum_{j=1}^{n} \vec{k}_{\perp j} \right) \\ &\times \psi^{\uparrow\,*}_{(n)}(x'_i, \vec{k}'_{\perp i}, \lambda_i) \ \psi^{\uparrow}_{(n)}(x_i, \vec{k}_{\perp i}, \lambda_i) (\sqrt{1-\zeta})^{1-n}, \end{aligned} \tag{52}$$

$$\sqrt{1-\zeta}\left(1+\frac{\zeta}{2(1-\zeta)}\right)\frac{(\Delta^1-\mathrm{i}\Delta^2)}{2M}f_{2\,(n\to n)}(x_1,t,\zeta)$$
$$=\sum_{n,\ \lambda}\prod_{i=1}^{n}\int_0^1 dx_{i(i\neq 1)}\int\frac{d^2\vec{k}_{\perp i}}{2(2\pi)^3}\ \delta\left(1-\sum_{j=1}^{n}x_j\right)\ \delta^{(2)}\left(\sum_{j=1}^{n}\vec{k}_{\perp j}\right)$$
$$\times\psi^{\uparrow\,*}_{(n)}(x_i',\vec{k}'_{\perp i},\lambda_i)\ \psi^{\downarrow}_{(n)}(x_i,\vec{k}_{\perp i},\lambda_i)(\sqrt{1-\zeta})^{1-n}, \tag{53}$$

where

$$\begin{cases} x_1'=\frac{x_1-\zeta}{1-\zeta}\,,\ \ \vec{k}'_{\perp 1}=\vec{k}_{\perp 1}-\frac{1-x_1}{1-\zeta}\vec{\Delta}_\perp \text{ for the struck quark,} \\ x_i'=\frac{x_i}{1-\zeta}\,,\ \ \ \vec{k}'_{\perp i}=\vec{k}_{\perp i}+\frac{x_i}{1-\zeta}\vec{\Delta}_\perp \ \ \text{for the } (n-1) \text{ spectators.}\end{cases} \tag{54}$$

A sum over all possible helicities λ_i is understood. If quark masses are neglected, the currents conserve helicity. We also can check that $\sum_{i=1}^n x_i'=1$, $\sum_{i=1}^n \vec{k}'_{\perp i}=\vec{0}_\perp$.

For the $n+1\to n-1$ off-diagonal term ($\Delta n=-2$), let us consider the case where partons 1 and $n+1$ of the initial wavefunction annihilate into the current leaving $n-1$ spectators. Then $x_{n+1}=\zeta-x_1$, $\vec{k}_{\perp n+1}=\vec{\Delta}_\perp-\vec{k}_{\perp 1}$. The remaining $n-1$ partons have total momentum $((1-\zeta)P^+,-\vec{\Delta}_\perp)$. The final wavefunction then has arguments $x_i'=\frac{x_i}{1-\zeta}$ and $\vec{k}'_{\perp i}=\vec{k}_{\perp i}+\frac{x_i}{1-\zeta}\vec{\Delta}_\perp$. We thus obtain the formulae for the off-diagonal matrix element of the Compton amplitude in the domain $0\le x_1\le\zeta$:

$$\sqrt{1-\zeta}f_{1\,(n+1\to n-1)}(x_1,t,\zeta)\ -\ \frac{\zeta^2}{4\sqrt{1-\zeta}}f_{2\,(n+1\to n-1)}(x_1,t,\zeta)$$
$$=\sum_{n,\ \lambda}\int_0^1 dx_{n+1}\int\frac{d^2\vec{k}_{\perp 1}}{2(2\pi)^3}\int\frac{d^2\vec{k}_{\perp n+1}}{2(2\pi)^3}\prod_{i=2}^{n}\int_0^1 dx_i\int\frac{d^2\vec{k}_{\perp i}}{2(2\pi)^3}$$
$$\times\delta\left(1-\sum_{j=1}^{n+1}x_j\right)\ \delta^{(2)}\left(\sum_{j=1}^{n+1}\vec{k}_{\perp j}\right)[\sqrt{1-\zeta}]^{1-n}$$
$$\times\psi^{\uparrow\,*}_{(n-1)}(x_i',\vec{k}'_{\perp i},\lambda_i)\ \psi^{\uparrow}_{(n+1)}(\{x_1,x_i,x_{n+1}=\zeta-x_1\},$$
$$\{\vec{k}_{\perp 1},\vec{k}_{\perp i},\vec{k}_{\perp n+1}=\vec{\Delta}_\perp-\vec{k}_{\perp 1}\},\{\lambda_1,\lambda_i,\lambda_{n+1}=-\lambda_1\}), \tag{55}$$

$$\sqrt{1-\zeta}\left(1+\frac{\zeta}{2(1-\zeta)}\right)\frac{(\Delta^1-\mathrm{i}\Delta^2)}{2M}f_{2\,(n+1\to n-1)}(x_1,t,\zeta)$$
$$=\sum_{n,\ \lambda}\int_0^1 dx_{n+1}\int\frac{d^2\vec{k}_{\perp 1}}{2(2\pi)^3}\int\frac{d^2\vec{k}_{\perp n+1}}{2(2\pi)^3}\prod_{i=2}^{n}\int_0^1 dx_i\int\frac{d^2\vec{k}_{\perp i}}{2(2\pi)^3}$$
$$\times\delta\left(1-\sum_{j=1}^{n+1}x_j\right)\ \delta^{(2)}\left(\sum_{j=1}^{n+1}\vec{k}_{\perp j}\right)[\sqrt{1-\zeta}]^{1-n}$$

$$\times \psi^{\uparrow\ *}_{(n-1)}(x'_i, \vec{k}'_{\perp i}, \lambda_i)\ \psi^{\downarrow}_{(n+1)}(\{x_1, x_i, x_{n+1} = \zeta - x_1\},$$

$$\{\vec{k}_{\perp 1}, \vec{k}_{\perp i}, \vec{k}_{\perp n+1} = \vec{\Delta}_\perp - \vec{k}_{\perp 1}\}, \{\lambda_1, \lambda_i, \lambda_{n+1} = -\lambda_1\}), \tag{56}$$

where $i = 2, 3, \cdots, n$ label the $n-1$ spectator partons which appear in the final-state hadron wavefunction with

$$x'_i = \frac{x_i}{1-\zeta}\,, \qquad \vec{k}'_{\perp i} = \vec{k}_{\perp i} + \frac{x_i}{1-\zeta}\vec{\Delta}_\perp\ . \tag{57}$$

We can again check that the arguments of the final-state wavefunction satisfy $\sum_{i=2}^n x'_i = 1$, $\sum_{i=2}^n \vec{k}'_{\perp i} = \vec{0}_\perp$.

The above representation is the general form for the generalized form factors of the deeply virtual Compton amplitude for any composite system. Thus given the light-cone Fock state wavefunctions of the eigensolutions of the light-cone Hamiltonian, we can compute the amplitude for virtual Compton scattering including all spin correlations. The formulae are accurate to leading order in $1/Q^2$. Radiative corrections to the quark Compton amplitude of order $\alpha_s(Q^2)$ from diagrams in which a hard gluon interacts between the two photons have also been neglected.

8 Electroweak Matrix Elements and Light-Cone Wavefunctions

Another remarkable advantage of the light-cone formalism is that exclusive semileptonic B-decay amplitudes such as $B \to A\ell\overline{\nu}$ can be evaluated exactly.[67] The time-like decay matrix elements require the computation of the diagonal matrix element $n \to n$ where parton number is conserved, and the off-diagonal $n+1 \to n-1$ convolution where the current operator annihilates a $q\overline{q'}$ pair in the initial B wavefunction. See Fig. 4. This term is a consequence of the fact that the time-like decay $q^2 = (p_\ell + p_{\overline{\nu}})^2 > 0$ requires a positive light-cone momentum fraction $q^+ > 0$. Conversely for space-like currents, one can choose $q^+ = 0$, as in the Drell-Yan-West representation of the space-like electromagnetic form factors. However, as can be seen from the explicit analysis of the form factor in a perturbative model, the off-diagonal convolution can yield a nonzero q^+/q^+ limiting form as $q^+ \to 0$. This extra term appears specifically in the case of "bad" currents such as J^- in which the coupling to $q\overline{q}$ fluctuations in the light-cone wavefunctions are favored. In effect, the $q^+ \to 0$ limit generates $\delta(x)$ contributions as residues of the $n+1 \to n-1$ contributions. The necessity for such "zero mode" $\delta(x)$ terms has been noted by Chang, Root and Yan [68], Burkardt [69], and Ji and Choi.[70]

The off-diagonal $n+1 \to n-1$ contributions give a new perspective for the physics of B-decays. A semileptonic decay involves not only matrix elements where a quark changes flavor, but also a contribution where the leptonic pair is created

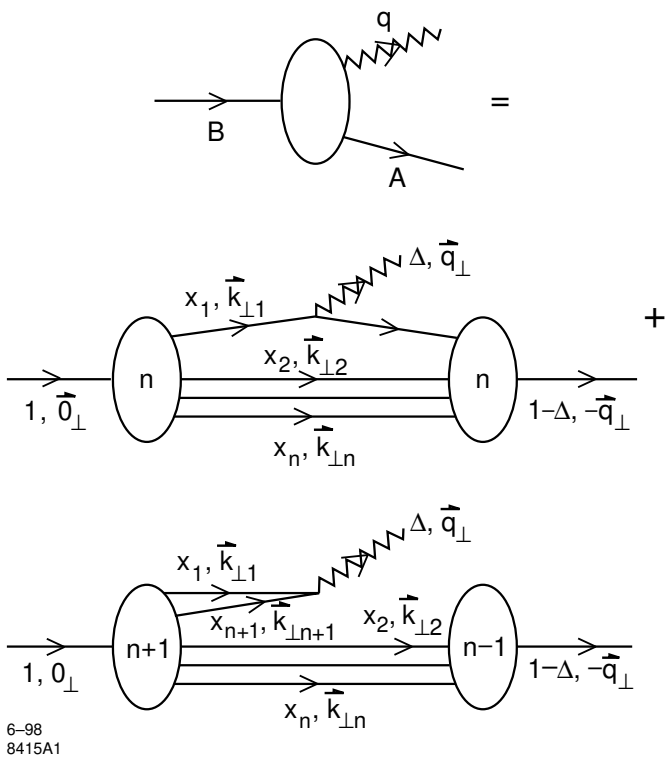

Figure 4: Exact representation of electroweak decays and time-like form factors in the light-cone Fock representation.

from the annihilation of a $q\overline{q'}$ pair within the Fock states of the initial B wavefunction. The semileptonic decay thus can occur from the annihilation of a nonvalence quark-antiquark pair in the initial hadron. This feature will carry over to exclusive hadronic B-decays, such as $B^0 \to \pi^- D^+$. In this case the pion can be produced from the coalescence of a $d\overline{u}$ pair emerging from the initial higher particle number Fock wavefunction of the B. The D meson is then formed from the remaining quarks after the internal exchange of a W boson.

In principle, a precise evaluation of the hadronic matrix elements needed for B-decays and other exclusive electroweak decay amplitudes requires knowledge of all of the light-cone Fock wavefunctions of the initial and final state hadrons. In the case of model gauge theories such as QCD(1+1) [71] or collinear QCD [72] in one-space and one-time dimensions, the complete evaluation of the light-cone wavefunction is possible for each baryon or meson bound-state using the DLCQ method. It would be interesting to use such solutions as a model for physical B-decays.

9 Applications of Light-Cone Factorization to Hard QCD Processes

Factorization theorems for hard exclusive, semi-exclusive, and diffractive processes allow a rigorous separation of soft non-perturbative dynamics of the bound state hadrons from the hard dynamics of a perturbatively-calculable quark-gluon scattering amplitude.

The light-cone formalism provides a physical factorization scheme which conveniently separates and factorizes soft non-perturbative physics from hard perturbative dynamics in both exclusive and inclusive reactions.[73, 74] In hard inclusive reactions all intermediate states are divided according to $\mathcal{M}_n^2 < \Lambda^2$ and $\mathcal{M}_n^2 > \Lambda^2$ domains. The lower mass regime is associated with the quark and gluon distributions defined from the absolute squares of the LC wavefunctions in the light cone factorization scheme. In the high invariant mass regime, intrinsic transverse momenta can be ignored, so that the structure of the process at leading power has the form of hard scattering on collinear quark and gluon constituents, as in the parton model. The attachment of gluons from the LC wavefunction to a propagator in a hard subprocess is power-law suppressed in LC gauge, so that the minimal quark-gluon particle-number subprocesses dominate. It is then straightforward to derive the DGLAP equations from the evolution of the distributions with $\log \Lambda^2$. The anomaly contribution to singlet helicity structure function $g_1(x, Q)$ can be explicitly identified in the LC factorization scheme as due to the $\gamma^* g \to q\overline{q}$ fusion process. The anomaly contribution would be zero if the gluon is on shell. However, if the off-shellness of the state is larger than the quark pair mass, one obtains the usual anomaly contribution.[75]

In exclusive amplitudes, the LC wavefunctions are the interpolating functions between the quark and gluon states and the hadronic states. In an exclusive amplitude involving a hard scale Q^2 all intermediate states can be divided according to $\mathcal{M}_n^2 < \Lambda^2 < Q^2$ and $\mathcal{M}_n^2 < \Lambda^2$ invariant mass domains. The high invariant mass contributions to the amplitude has the structure of a hard scattering process T_H in which the hadrons are replaced by their respective (collinear) quarks and gluons. In light-cone gauge only the minimal Fock states contribute to the leading power-law fall-off of the exclusive amplitude. The wavefunctions in the lower invariant mass domain can be integrated up to the invariant mass cutoff Λ. Final-state and initial state corrections from gluon attachments to lines connected to the color-singlet distribution amplitudes cancel at leading twist.

Given the solution for the hadronic wavefunctions $\psi_n^{(\Lambda)}$ with $\mathcal{M}_n^2 < \Lambda^2$, one can construct the wavefunction in the hard regime with $\mathcal{M}_n^2 > \Lambda^2$ using projection operator techniques.[76] The construction can be done perturbatively in QCD since only high invariant mass, far off-shell matrix elements are involved. One can use this method to derive the physical properties of the LC wavefunctions and their matrix elements at high invariant mass. Since $\mathcal{M}_n^2 = \sum_{i=1}^n \left(\frac{k_\perp^2 + m^2}{x}\right)_i$, this method also allows the derivation of the asymptotic behavior of light-cone wavefunctions at large $k_\perp$,

which in turn leads to predictions for the fall-off of form factors and other exclusive matrix elements at large momentum transfer, such as the quark counting rules for predicting the nominal power-law fall-off of two-body scattering amplitudes at fixed θ_{cm}.[7] The phenomenological successes of these rules can be understood within QCD if the coupling $\alpha_V(Q)$ freezes in a range of relatively small momentum transfer.[77]

The key non-perturbative input for exclusive processes is the gauge and frame independent hadron distribution amplitude [74, 73] defined as the integral of the valence (lowest particle number) Fock wavefunction; *e.g.* for the pion

$$\phi_\pi(x_i, \Lambda) \equiv \int d^2 k_\perp \, \psi^{(\Lambda)}_{q\bar{q}/\pi}(x_i, \vec{k}_{\perp i}, \lambda) \tag{58}$$

where the global cutoff Λ is identified with the resolution Q. The distribution amplitude controls leading-twist exclusive amplitudes at high momentum transfer, and it can be related to the gauge-invariant Bethe-Salpeter wavefunction at equal light-cone time. The logarithmic evolution of hadron distribution amplitudes $\phi_H(x_i, Q)$ can be derived from the perturbatively-computable tail of the valence light-cone wavefunction in the high transverse momentum regime.[74, 73] The conformal basis for the evolution of the three-quark distribution amplitudes for the baryons [78] has recently been obtained by V. Braun *et al.*[16]

Thus at high transverse momentum an exclusive amplitudes factorizes into a convolution of a hard quark-gluon subprocess amplitudes T_H with the hadron distribution amplitudes $\phi(x_i, \Lambda)$.[4] The T_H satisfy the dimensional counting rules. The logarithmic evolution of hadron distribution amplitudes $\phi_H(x_i, Q)$ can be derived from the perturbatively-computable tail of the valence light-cone wavefunction in the high transverse momentum regime.[76]

The existence of an exact formalism provides a basis for systematic approximations and a control over neglected terms. For example, one can analyze exclusive semi-leptonic B-decays which involve hard internal momentum transfer using a perturbative QCD formalism[79, 80] patterned after the analysis of form factors at large momentum transfer.[76] The hard-scattering analysis again proceeds by writing each hadronic wavefunction as a sum of soft and hard contributions

$$\psi_n = \psi_n^{\rm soft}(\mathcal{M}_n^2 < \Lambda^2) + \psi_n^{\rm hard}(\mathcal{M}_n^2 > \Lambda^2), \tag{59}$$

where $\mathcal{M}_n^2$ is the invariant mass of the partons in the n-particle Fock state and Λ is the separation scale. The high internal momentum contributions to the wavefunction $\psi_n^{\rm hard}$ can be calculated systematically from QCD perturbation theory by iterating the gluon exchange kernel. The contributions from high momentum transfer exchange to the B-decay amplitude can then be written as a convolution of a hard-scattering quark-gluon scattering amplitude T_H with the distribution amplitudes $\phi(x_i, \Lambda)$, the valence wavefunctions obtained by integrating the constituent momenta up to the separation scale $\mathcal{M}_n < \Lambda < Q$. Furthermore in processes such as $B \to \pi D$ where the pion is effectively produced as a rapidly-moving small Fock state with a small

color-dipole interactions, final state interactions are suppressed by color transparency. This is the basis for the perturbative hard-scattering analyses.[79, 81, 82, 80] In the exact analysis, one can identify the hard PQCD contribution as well as the soft contribution from the convolution of the light-cone wavefunctions. Furthermore, the hard-scattering contribution can be systematically improved.

10 Non-Perturbative Solutions of Light-Cone Quantized QCD

It is clearly important not only to compute the spectrum of hadrons and gluonic states, but also to determine the wavefunction of each QCD bound state in terms of its fundamental quark and gluon degrees of freedom. If we could obtain such nonperturbative solutions of QCD, then we could compute the quark and gluon structure functions and distribution amplitudes which control hard-scattering inclusive and exclusive reactions as well as calculate the matrix elements of currents which underlie electroweak form factors and the weak decay amplitudes of the light and heavy hadrons. The light-cone wavefunctions also determine the multi-parton correlations which control the distribution of particles in the proton fragmentation region as well as dynamical higher twist effects. Thus one can analyze not only the deep inelastic structure functions but also the fragmentation of the spectator system. Knowledge of hadron wavefunctions would also open a window to a deeper understanding of the physics of QCD at the amplitude level, illuminating exotic effects of the theory such as color transparency, intrinsic heavy quark effects, hidden color, diffractive processes, and the QCD van der Waals interactions.

Is there any hope of computing light-cone wavefunctions from first principles? In the discretized light-cone quantization method (DLCQ),[83] periodic boundary conditions are introduced in $b_\perp$ and x^- so that the momenta $k_{\perp i} = n_\perp \pi / L_\perp$ and $x_i^+ = n_i/K$ are discrete. A global cutoff in invariant mass of the partons in the Fock expansion is also introduced. Solving the quantum field theory then reduces to the problem of diagonalizing the finite-dimensional hermitian matrix H_{LC} on a finite discrete Fock basis. The DLCQ method has now become a standard tool for solving both the spectrum and light-cone wavefunctions of one-space one-time theories – virtually any $1+1$ quantum field theory, including "reduced QCD" (which has both quark and gluonic degrees of freedom) can be completely solved using DLCQ.[84, 85, 72] The method yields not only the bound-state and continuum spectrum, but also the light-cone wavefunction for each eigensolution. The solutions for the model 1+1 theories can provide an important theoretical laboratory for testing approximations and QCD-based models.

In the case of theories in 3+1 dimensions, Hiller, McCartor, and I [48, 86] have recently shown that the use of covariant Pauli-Villars regularization with DLCQ allows one to obtain the spectrum and light-cone wavefunctions of simplified theories, such as (3+1) Yukawa theory. Dalley *et al.* have shown how one can use DLCQ in one

space-one time, with a transverse lattice to solve mesonic and gluonic states in $3+1$ QCD.[87] The spectrum obtained for gluonium states is in remarkable agreement with lattice gauge theory results, but with a huge reduction of numerical effort. Hiller and I [88] have shown how one can use DLCQ to compute the electron magnetic moment in QED without resort to perturbation theory. Light-cone gauge $A^+ = 0$ allows one to utilize only the physical degrees of freedom of the gluon field to appear. However, light-cone quantization in Feynman gauge has a number of attractive features, including manifest covariance and a straightforward passage to the Coulomb limit in the case of static quarks.[89]

One can also formulate DLCQ so that supersymmetry is exactly preserved in the discrete approximation, thus combining the power of DLCQ with the beauty of supersymmetry.[90, 91, 92] The "SDLCQ" method has been applied to several interesting supersymmetric theories, to the analysis of zero modes, vacuum degeneracy, massless states, mass gaps, and theories in higher dimensions, and even tests of the Maldacena conjecture.[90]

Broken supersymmetry is interesting in DLCQ, since it may serve as a method for regulating non-Abelian theories.[86] Another remarkable advantage of light-cone quantization is that the vacuum state $|0\rangle$ of the full QCD Hamiltonian coincides with the free vacuum. For example, as discussed by Bassetto,[93] the computation of the spectrum of $QCD(1+1)$ in equal time quantization requires constructing the full spectrum of non perturbative contributions (instantons). However, light-cone methods with infrared regularization give the correct result without any need for vacuum-related contributions. The role of instantons and such phenomena in light-cone quantized $QCD(3+1)$ is presumably more complicated and may reside in zero modes; [94] *e.g.*, zero modes are evidently necessary to represent theories with spontaneous symmetry breaking.[95]

Light-cone wavefunctions thus are the natural quantities to encode hadron properties and to bridge the gap between empirical constraints and theoretical predictions for the bound state solutions. We can thus envision a program to construct the hadronic light cone Fock wavefunctions $\psi_n(x_i, k_{\perp i}, \lambda_i)$ using not only data but constraints such as:

(1) Since the state is far off shell at large invariant mass $\mathcal{M}$, one can derive rigorous limits on the $x \to 1$, high $k_\perp$, and high $\mathcal{M}_n^2$ behavior of the wavefunctions in the perturbative domain.

(2) Ladder relations connecting state of different particle number follow from the QCD equation of motion and lead to Regge behavior of the quark and gluon distributions at $x \to 0$. QED provides a constraint at $N_C \to 0$.

(3) One can obtain guides to the exact behavior of LC wavefunctions in QCD from analytic or DLCQ solutions to toy models such as "reduced" $QCD(1+1)$.

(4) QCD sum rules, lattice gauge theory moments, and QCD inspired models such as the bag model, chiral theories, provide important constraints. An important question is how the light-cone wavefunctions incorporate chiral constraints such as soliton (Skyrmion) behavior for baryons and other consequences of the chiral limit.

However it has been shown that the anomaly contribution for the $\pi^0 \to \gamma\gamma$ decay amplitude is satisfied by the light-cone Fock formalism in the limit where the mass of the pion is light compared to its size.[139]

(5) Since the LC formalism is valid at all scales, one can utilize empirical constraints such as the measurements of magnetic moments, axial couplings, form factors, and distribution amplitudes.

(6) In the nonrelativistic limit, the light-cone and many-body Schrödinger theory formalisms must match.

11 Self-Resolved Diffractive Reactions and Light Cone Wavefunctions

Diffractive multi-jet production in heavy nuclei provides a novel way to measure the shape of the LC Fock state wavefunctions and test color transparency. For example, consider the reaction [96, 97, 98] $\pi A \to \text{Jet}_1 + \text{Jet}_2 + A'$ at high energy where the nucleus A' is left intact in its ground state. The transverse momenta of the jets balance so that $\vec{k}_{\perp i} + \vec{k}_{\perp 2} = \vec{q}_\perp < R^{-1}{}_A$. The light-cone longitudinal momentum fractions also need to add to $x_1 + x_2 \sim 1$ so that $\Delta p_L < R_A^{-1}$. The process can then occur coherently in the nucleus. Because of color transparency, the valence wavefunction of the pion with small impact separation, will penetrate the nucleus with minimal interactions, diffracting into jet pairs.[96] The $x_1 = x$, $x_2 = 1 - x$ dependence of the di-jet distributions will thus reflect the shape of the pion valence light-cone wavefunction in x; similarly, the $\vec{k}_{\perp 1} - \vec{k}_{\perp 2}$ relative transverse momenta of the jets gives key information on the derivative of the underlying shape of the valence pion wavefunction.[97, 98, 99] The diffractive nuclear amplitude extrapolated to $t = 0$ should be linear in nuclear number A if color transparency is correct. The integrated diffractive rate should then scale as $A^2/R_A^2 \sim A^{4/3}$. Preliminary results on a diffractive dissociation experiment of this type E791 at Fermilab using 500 GeV incident pions on nuclear targets.[13] appear to be consistent with color transparency.[13] The momentum fraction distribution of the jets is consistent with a valence light-cone wavefunction of the pion consistent with the shape of the asymptotic distribution amplitude, $\phi_\pi^{\text{asympt}}(x) = \sqrt{3} f_\pi x(1-x)$. Data from CLEO [100] for the $\gamma\gamma^* \to \pi^0$ transition form factor also favor a form for the pion distribution amplitude close to the asymptotic solution [74, 73] to the perturbative QCD evolution equation.

The diffractive dissociation of a hadron or nucleus can also occur via the Coulomb dissociation of a beam particle on an electron beam (*e.g.* at HERA or eRHIC) or on the strong Coulomb field of a heavy nucleus (*e.g.* at RHIC or nuclear collisions at the LHC).[99] The amplitude for Coulomb exchange at small momentum transfer is proportional to the first derivative $\sum_i e_i \frac{\partial}{\vec{k}_{Ti}} \psi$ of the light-cone wavefunction, summed over the charged constituents. The Coulomb exchange reactions fall off less fast at high transverse momentum compared to pomeron exchange reactions since the light-

cone wavefunction is effective differentiated twice in two-gluon exchange reactions.

It will also be interesting to study diffractive tri-jet production using proton beams $pA \to \text{Jet}_1 + \text{Jet}_2 + \text{Jet}_3 + A'$ to determine the fundamental shape of the 3-quark structure of the valence light-cone wavefunction of the nucleon at small transverse separation.[97] For example, consider the Coulomb dissociation of a high energy proton at HERA. The proton can dissociate into three jets corresponding to the three-quark structure of the valence light-cone wavefunction. We can demand that the produced hadrons all fall outside an opening angle θ in the proton's fragmentation region. Effectively all of the light-cone momentum $\sum_j x_j \simeq 1$ of the proton's fragments will thus be produced outside an "exclusion cone". This then limits the invariant mass of the contributing Fock state $\mathcal{M}_n^2 > \Lambda^2 = P^{+2} \sin^2\theta/4$ from below, so that perturbative QCD counting rules can predict the fall-off in the jet system invariant mass $\mathcal{M}$. At large invariant mass one expects the three-quark valence Fock state of the proton to dominate. The segmentation of the forward detector in azimuthal angle ϕ can be used to identify structure and correlations associated with the three-quark light-cone wavefunction.[99] An interesting possibility is that the distribution amplitude of the $\Delta(1232)$ for $J_z = 1/2, 3/2$ is close to the asymptotic form $x_1 x_2 x_3$, but that the proton distribution amplitude is more complex. This ansatz can also be motivated by assuming a quark-diquark structure of the baryon wavefunctions. The differences in shapes of the distribution amplitudes could explain why the $p \to \Delta$ transition form factor appears to fall faster at large Q^2 than the elastic $p \to p$ and the other $p \to N^*$ transition form factors.[101] One can use also measure the dijet structure of real and virtual photons beams $\gamma^* A \to \text{Jet}_1 + \text{Jet}_2 + A'$ to measure the shape of the light-cone wavefunction for transversely-polarized and longitudinally-polarized virtual photons. Such experiments will open up a direct window on the amplitude structure of hadrons at short distances. The light-cone formalism is also applicable to the description of nuclei in terms of their nucleonic and mesonic degrees of freedom.[102, 103] Self-resolving diffractive jet reactions in high energy electron-nucleus collisions and hadron-nucleus collisions at moderate momentum transfers can thus be used to resolve the light-cone wavefunctions of nuclei.

12 Dynamical Correlations and Higher-Twist Effects in QCD

It is an empirical fact that conventional leading twist contributions cannot account for the measured $ep \to eX$ and $ed \to eX$ structure functions at $x \gtrsim 0.4$ and $Q^2 \lesssim 5$ GeV^2. Fits to the data [104, 105] require an additional component which scales as $1/Q^2$ relative to the leading twist contributions and rises rapidly with x. The excess contribution can be parameterized in the form

$$F_{2p,n}(x, Q^2) = F^0_{2p,n}(x, Q^2) \left[1 + \frac{c^{p,n}_{HT}(x)}{Q^2} \right] \tag{60}$$

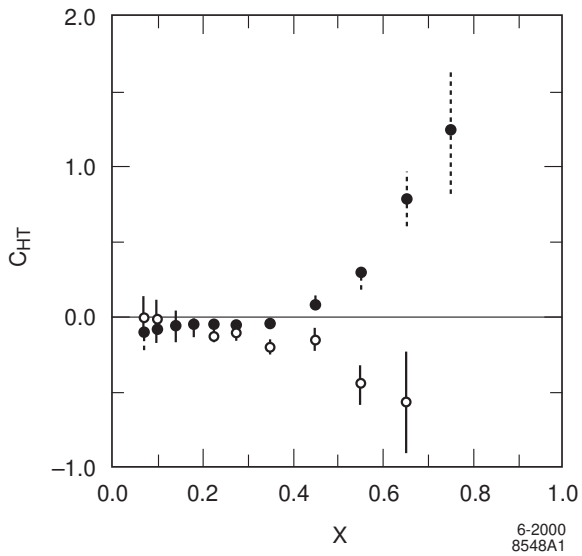

Figure 5: Higher-twist coefficients $C_{HT}(x)$ [in GeV^2 units] for inelastic lepton scattering on proton target (solid points) and the difference $C^p_{HT}(x) - C^n_{HT}(x)$ for proton minus neutron targets (open circles).[104, 105] The data compilation is taken from Souder.[108]

where $F^0_{2p,n}$ is the leading twist contribution. The functional dependence of the higher-twist term $C^{p,n}_{HT}(x)$ for proton and proton-neutron targets is shown in Fig. 5. A rough fit is

$$c^p_{HT}(x) \cong \left[\frac{0.3\ GeV}{1-x}\right]^2 \qquad c^n_{HT}(x) \cong 2c^p_{HT}(x)\ ; \tag{61}$$

i.e.: the higher-twist effect relative to the leading twist contribution for the neutron is stronger than that of the proton.

A possible source of higher-twist effects in PQCD is "renormalons".[106, 107] This contribution to the deep inelastic lepton-hadron cross section reflects a divergent $\beta^n_0\, n!$ growth of the PQCD series for hard radiative corrections to deep inelastic scattering evolution at high orders in $\alpha^n_s(Q^2)$. The factorial growth arises from the integration over the QCD running coupling; *i.e.*, the summation of the reducible multi-bubble loop-diagrams in the gluon propagator. The net effect is to correct the leading twist predictions by a power-law suppressed $1/Q^2(1-x)$ contribution. Alternatively, one can proceed using the BLM method [109]: one first identifies the conformal coefficients[21] of the PQCD series; by definition these are independent of the $\beta-$function and are hence devoid of the $\beta^n_0\, n!$ growth. The scale of the running coupling is set by requiring that all of the β-dependence resides in $\alpha_s(Q^{*2})$. The resulting scale $(Q^{*2}) \propto (1-x)Q^2$ can also be understood as the mean value of the argument of the running coupling $\alpha_s(k^2)$ in the Feynman loop integration.

However, the renormalon contribution cannot account for the observed higher-twist contribution shown in Fig. 5 since it is proportional to the leading-twist prediction, *i.e.*: $c^p_{HTren}(x) = c^n_{HTren}(x)$. Thus it is apparent from the data that there must be a dynamical origin for the observed $C_{HT}(x)/Q^2$ contribution. In fact, dynamical higher-twist terms naturally arise from multi-parton correlations. For example, if the electron recoils against 1, 2, or 3 quarks, one obtains a series of higher-twist contributions of ascending order in $1/Q^2$.

$$\begin{aligned} \sigma_T &\sim \frac{(1-x)^3}{Q^2)} \qquad eq \to eq \\ \sigma_L &\sim \frac{(1-x)}{(Q^2)^3} \qquad eqq \to eqq \\ \sigma_T &\sim \frac{1}{(1-x)}\left(\frac{1}{Q^2}\right)^3 \qquad eqqq \to eqqq \end{aligned} \tag{62}$$

where the extra $1/Q^2$ fall-off reflects the form factor squared of the (qq) or (qqq) systems, and the enhancement at $x \to 1$ reflects the fact that the (qq) and (qqq) composites carry increasing fractions of the proton light-cone momentum. The dominance of σ_L for $eqq \to eqq$ reflects the bosonic coupling of the composite di-quark. Each of the contributions satisfy Bloom-Gilman duality [110] at fixed W^2. The multi-parton subprocesses are suppressed by powers of $1/Q^2$ but enhanced at large x since more of the momentum of the target proton is fed into the hard subprocess; *i.e.*, there are fewer spectators to stop. The general rule is

$$F_2(x, Q^2) \propto \frac{(1-x)^{2n_{spect}-1+2\Delta h}}{Q^{n_{active}-4}} \tag{63}$$

where n is the number of partons or other quanta participating in the hard subprocess and Δh is the difference in helicity between the active partons and the target.[111]

It is well-known that higher-twist, power-law suppressed corrections to hard inclusive cross sections can be a signature of correlation effects involving two or more valence quarks of a hadron. For example, the lepton angular dependence of the leading-twist PQCD prediction for Drell Yan lepton pair production $d\sigma(\pi A \to \ell^+\ell^- X)/d\Omega$ is $1 + \cos^2\theta_{cm}$. The data[112, 113] however shows the onset of $\sin^2\theta_{cm}$ dependence at large x_F. This signals the presence of multiparton-induced subprocesses such as $(\overline{q}q)q \to \gamma^*(Q^2)q \to \ell^+\ell^- q$.[114] See Fig. 6. Such reactions produce longitudinally-polarized virtual photons with a $\sin^2\theta_{cm}$ lepton pair angular dependence in contrast to the transversally polarized Drell-Yan pairs produced from the $\overline{q}q \to \gamma^*(Q^2) \to \ell^+\ell^-$ subprocess. The penalty for utilizing the two correlated partons in the pion wave-function is an extra suppression factor $1/R^2Q^2(1-x_F)^2$ where R is the characteristic interquark transverse separation between the valence quarks in the incoming meson. The origin of the $1/R^2Q^2$ scaling is similar to that of the photon to meson transition

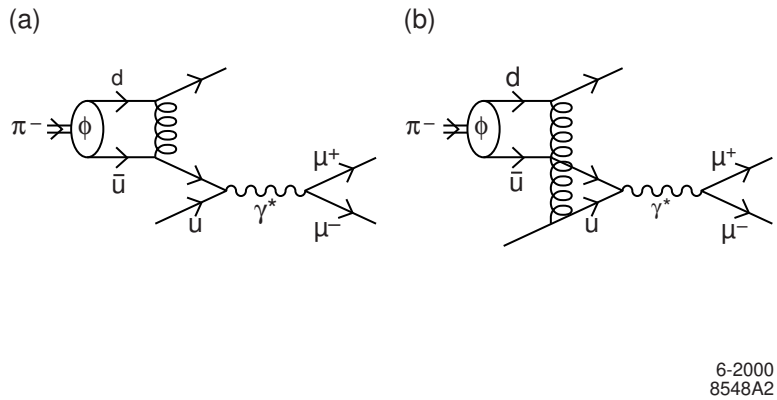

Figure 6: Higher-twist contribution to lepton pair production in πN scattering. The dynamics at large x_F requires both constituents of the projectile meson to be involved in the hard subprocess. [115]

form factor in the exclusive reaction $\ell\gamma \to \ell(\overline{q}q) \to \pi^0$.[4] The scale $1/R$ can be related to the pion decay constant f_π which normalizes the pion distribution amplitude.[4] At fixed Q^2 the higher-twist process can actually dominate as $x_F \to 1$ since all of the incoming momentum of the pion is transferred to the subprocess. The correlated subprocess $(\overline{q}q)q \to \gamma^*(Q^2)q \to \ell^+\ell^-q$ also leads to the prediction of $\sin^2\theta\cos 2\phi$ and $\sin 2\theta\cos\phi$ terms in the angular distribution[115], effects which are clearly apparent in the data. [112, 113]

Another important example of dynamical higher-twist effects is the reaction $\pi A \to J/\psi X$ which is observed to produce longitudinally-polarized $J/\psi's$ at large x_F.[116] Again this effect can be attributed to highly correlated multi-parton subprocesses such as $\overline{q}qg \to \overline{c}c\overline{q}q$ where both valence quarks of the incident pion must be involved in the hard subprocess in order to produce the charmed quark pair with nearly all of the incident momentum of the incoming meson.[117] Similarly, charm production at threshold requires that all of the momentum of the target nucleon be transferred to the charm quarks. In the $\gamma p \to c\overline{c}p$ reaction near threshold, all the partons have to transfer their energy to the charm quarks within their reaction time $1/m_c$, and must be within this transverse distance from the $c\overline{c}$ and from each other. Hence only compact Fock states of the target nucleon or nucleus with a radius equal to the Compton wavelength of the heavy quark, can contribute to charm production at threshold. Equivalently we can interpret the multi-connected charm quarks as intrinsic charm Fock states which are kinematically favored to have large momentum fractions.[118] The experimental evidence for intrinsic charm is discussed by Harris, Smith, and Vogt.[119]

Near-threshold charm production also probes the $x \simeq 1$ configurations in the target wavefunction; the spectator partons carry a vanishing fraction $x \simeq 0$ of the target

momentum. This implies that the production rate behaves near $x \to 1$ approximately as $(1-x)^{2n_s-1}$ where n_s is the number of spectators required to stop. Including spin factors, we can identify three different gluonic components of the photoproduction cross-section:

- The usual one-gluon $(1-x)^4$ distribution for leading twist photon-gluon fusion $\gamma g \to c\overline{c}$, which leaves two quarks spectators;
- Two correlated gluons emitted from the proton with a net distribution $(1-x)^2/R^2\mathcal{M}^2$ for $\gamma gg \to c\overline{c}$, leaving one quark spectator;
- Three correlated gluons emitted from the proton with a net distribution $(1-x)^0/R^4\mathcal{M}^4$ for $\gamma ggg \to c\overline{c}$, leaving no quark spectators.

Here $x \approx \mathcal{M}^2/(s-m^2)$ and $\mathcal{M}$ is the mass of the $c\overline{c}$ pair. The relative weight of the multiply-connected terms is controlled by the inter-quark separation $R \simeq 1/m_c$. The extra powers of $1/\mathcal{M}$ arise from the power-law fall-off of the higher-twist hard subprocesses.[120]

The correlations between valence quarks can also have an important effect in deep inelastic scattering, particularly at large $x_{bj} = Q^2/2p \cdot q$. As noted above, one expects a sum of contributions to the deep inelastic cross section scaling nominally as

$$F_2(x,Q^2) = A(1-x)^3 + B\frac{(1-x)^2}{Q^4} + C\frac{(1-x)^{-1}}{Q^8} \tag{64}$$

corresponding to the subprocesses $\ell q \to \ell q$, $\ell(qq) \to \ell(qq)$, and $\ell(qqq) \to \ell(qqq)$. However, the above classification of terms in $F_2(x,Q^2)$ neglects what may be the most significant and interesting higher-twist contribution to deep inelastic scattering: the interference contributions. Let us consider the contribution to DIS due to the interference of the amplitude where the lepton scatters on one quark with the amplitude where the lepton scatters on another quark. See Fig. 7. One might think such contributions are assumed to be negligible since the hard subprocesses seem to lead to different non-interfering final states. Actually these contributions can interfere if the struck quarks have high internal momentum in the initial state or if they exchange large momenta in the final state. In either case, the apparently different final states can overlap. An insightful nuclear physics analog has been discussed by Drell.[121]

Let us consider the electroproduction subprocess $\ell(qq) \to \ell qq$ where the initial (qq) are collinear and have small invariant mass in the initial state and the qq pair in the final state can have large invariant mass. The lepton can effectively scatter on either quark. The nominal scaling of such twist-four contributions is

$$F_2^{\text{interference}}(x,Q^2) = \sum_{a\neq b} e_a e_b \frac{(1-x)^2}{R_{ab}^2 Q^2} \tag{65}$$

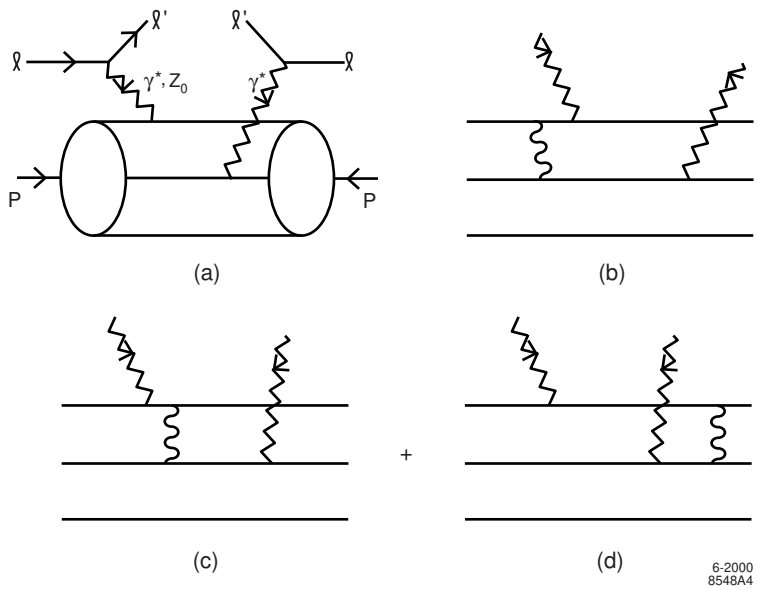

Figure 7: (a) Twist-four contribution to inelastic lepton scattering where the lepton scatters on different quarks. The interference of γ^* and Z^0 exchange contributions leads to parity and charge-conjugation violation of the higher-twist contribution. (b-d) The leading-order $\mathcal{O}(\alpha_s/Q^2R^2)$ perturbative QCD gluon-exchange contributions. The higher-twist contribution to the structure function is obtained by a convolution of the nucleon light-cone wavefunctions with the $\gamma^*(qq) \to \gamma^*(qq)$ multi-quark amplitude.

where the factor of $1/R_{ab}^2$ reflects the inter-parton distance. The interference terms are distinctive since, unlike renormalon contributions, they do not track with the leading twist contributions. The growth at high x of the twist-four process reflects the fact that the $\ell(qq) \to \ell qq$ subprocess incorporates the momentum of both quarks. This contribution must also play an important role in the physics of Bloom-Gilman duality [110] since the interference contributions also appear in square of the transition form factors. The interference terms can contribute to both F_L and F_T. There is an extensive literature on higher-twist contributions to the structure functions coming from such four-fermion operators.[122, 123] They are also referred to as "cat ear" diagrams from their appearance in the virtual Compton amplitude.

Let us suppose that the proton wavefunction is symmetric in the coordinates of the three valence quarks. If we sum over the pairs of valence quarks, we obtain a vanishing contribution on a proton target

$$\sum_{a\neq b} e_a e_b = (\sum_a e_a)^2 - \sum_a e_a^2 = 1 - (4/9 + 4/9 + 1/9) = 0. \tag{66}$$

However, for the neutron

$$\sum_{a\neq b} e_a e_b = (\sum_a e_a)^2 - \sum_a e_a^2 = 0 - (4/9 + 1/9 + 1/9) = 2/3. \tag{67}$$

Thus for symmetric nucleon wavefunctions the dynamical higher-twist cross terms appear to be are zero in the proton and significant for the neutron, deuteron, and nuclei! This is a very distinctive effect; it particularly motivates the empirical study of higher-twist effects using the deuteron and nuclear targets.

In a more realistic treatment, one needs to take into account correlation substructure. For example, suppose that we can approximate the nucleon wavefunctions as quark di-quark composites, where the di-quark has $I = 0$ and $J = 0$. Let us also suppose that the inter-quark separation R_{ab} is smallest for the two quarks of the diquark composite. In this case we can approximate the full sum as a sum over the quark charges of the $I = 0$ ud diquark. Then $\sum_{a\neq b} e_a e_b = e_u e_d = -2/9$ for both the proton and neutron targets. However, since it is conventional to parameterize the higher-twist contribution as a correction to the leading twist term. Thus $C_{p,n}(x)$ is predicted to rise strongly at large x and $C_n(x)$ will be larger than $C_p(x)$ since the leading-twist contribution to the neutron structure function $F_2^n(x, Q^2)$ is significantly smaller than $F_2^p(x, Q^2)$. These predictions seem consistent with the empirical higher-twist contributions to electroproduction extracted in the references.[104, 105] A simple test of the $I = 0$ diquark higher-twist model is the absence of twist-four contributions to the combination of structure functions $F_2^d(x, Q^2) - 2F_2^p(x, Q^2)$

It is also interesting to note that one can have interference between the amplitude for lepton-quark scattering via photon exchange on one quark with the amplitude for Z^0 exchange on another quark. This implies a distinctive parity-violating higher-twist contribution $C_{HT}^{PV}(x)$ proportional to the product of electromagnetic and weak quark charges $\sum_{a\neq b} e_a^\gamma e_b^{Z^0}$. Twist-four contributions of this type have been in fact been modeled [124] for structure function moments. However there is also the possibility of high-x enhancement. In fact, the x-dependence of $C_{HT}^{PV}(x)$ should be similar to the parity-conserving contribution.

We can also use Bloom-Gilman duality to predict that the parity-violating structure functions at large x should average to the contributions of the elastic and inelastic electroproduction channels when integrated over similar ranges in W^2. In fact, the parity-violating elastic form factors can be predicted at large momentum transfer in perturbative QCD.[125] Such measurements will provide very interesting tests of the applicability of PQCD to exclusive processes. Thus as emphasized by Souder [108], the detailed measurement of the left-right asymmetry A_{LR} in polarized elastic and inelastic electron-proton and polarized electron nucleus scattering at large x_{bj} can be a powerful illuminator of quark-quark correlations and fundamental QCD physics at the amplitude level.

13 Higher Fock States and the Intrinsic Sea

The main features of the heavy sea quark-pair contributions of the higher particle number Fock state states of light hadrons can be derived from perturbative QCD. One can identify two contributions to the heavy quark sea, the "extrinsic" contributions which correspond to ordinary gluon splitting, and the "intrinsic" sea which is multi-connected via gluons to the valence quarks. The leading $1/m_Q^2$ contributions to the intrinsic sea of the proton in the heavy quark expansion are proton matrix elements of the operator [126] $\eta^\mu \eta^\nu G_{\alpha\mu} G_{\beta\nu} G^{\alpha\beta}$ which in light-cone gauge $\eta^\mu A_\mu = A^+ = 0$ corresponds to three or four gluon exchange between the heavy-quark loop and the proton constituents in the forward virtual Compton amplitude. The intrinsic sea is thus sensitive to the hadronic bound-state structure.[127, 118] The maximal contribution of the intrinsic heavy quark occurs at $x_Q \simeq m_{\perp Q} / \sum_i m_\perp$ where $m_\perp = \sqrt{m^2 + k_\perp^2}$; *i.e.* at large x_Q, since this minimizes the invariant mass $\mathcal{M}_n^2$. The measurements of the charm structure function by the EMC experiment are consistent with intrinsic charm at large x in the nucleon with a probability of order $0.6 \pm 0.3\%$.[119] which is consistent with recent estimates based on instanton fluctuations.[126] Similarly, one can distinguish intrinsic gluons which are associated with multi-quark interactions and extrinsic gluon contributions associated with quark substructure.[128] One can also use this framework to isolate the physics of the anomaly contribution to the Ellis-Jaffe sum rule.[75] Thus neither gluons nor sea quarks are solely generated by DGLAP evolution, and one cannot define a resolution scale Q_0 where the sea or gluon degrees of freedom can be neglected.

It is usually assumed that a heavy quarkonium state such as the J/ψ always decays to light hadrons via the annihilation of its heavy quark constituents to gluons. However, as Karliner and I [129] have shown, the transition $J/\psi \to \rho\pi$ can also occur by the rearrangement of the $c\overline{c}$ from the J/ψ into the $\mid q\overline{q}c\overline{c}\rangle$ intrinsic charm Fock state of the ρ or π. On the other hand, the overlap rearrangement integral in the decay $\psi' \to \rho\pi$ will be suppressed since the intrinsic charm Fock state radial wavefunction of the light hadrons will evidently not have nodes in its radial wavefunction. This observation provides a natural explanation of the long-standing puzzle [130] why the J/ψ decays prominently to two-body pseudoscalar-vector final states, breaking hadron helicity conservation, [131] whereas the ψ' does not.

The higher Fock state of the proton $\mid uuds\overline{s}\rangle$ should resemble a $\mid K\Lambda\rangle$ intermediate state, since this minimizes its invariant mass $\mathcal{M}$. In such a state, the strange quark has a higher mean momentum fraction x than the $\overline{s}$.[132, 133, 134] Similarly, the helicity of the intrinsic strange quark in this configuration will be anti-aligned with the helicity of the nucleon.[132, 134] This $Q \leftrightarrow \overline{Q}$ asymmetry is a striking feature of the intrinsic heavy-quark sea.

14 Other Applications of Light-Cone Quantization to QCD Phenomenology

There are other phenomenological consequences of the light-cone Fock expansion:

Color Transparency. A crucial feature of the light-cone formalism is the fact that the form of the $\psi^{(\Lambda)}_{n/H}(x_i, \vec{k}_{\perp i}, \lambda_i)$ is invariant under longitudinal boosts; *i.e.*, the light-cone wavefunctions expressed in the relative coordinates x_i and $k_{\perp i}$ are independent of the total momentum P^+, $\vec{P}_\perp$ of the hadron. The ensemble $\{\psi_{n/H}\}$ of such light-cone Fock wavefunctions is a key concept for hadronic physics, providing a conceptual basis for representing physical hadrons (and also nuclei) in terms of their fundamental quark and gluon degrees of freedom. Each Fock state interacts distinctly; *e.g.*, Fock states with small particle number and small impact separation have small color dipole moments and can traverse a nucleus with minimal interactions. This is the basis for the predictions for "color transparency" in hard quasi-exclusive reactions.[10]

Diffractive vector meson photoproduction. The light-cone Fock wavefunction representation of hadronic amplitudes allows a simple eikonal analysis of diffractive high energy processes, such as $\gamma^*(Q^2)p \to \rho p$, in terms of the virtual photon and the vector meson Fock state light-cone wavefunctions convoluted with the $gp \to gp$ near-forward matrix element.[135] One can easily show that only small transverse size $b_\perp \sim 1/Q$ of the vector meson distribution amplitude is involved. The hadronic interactions are minimal, and thus the $\gamma^*(Q^2)N \to \rho N$ reaction can occur coherently throughout a nuclear target in reactions without absorption or shadowing. The $\gamma^* A \to VA$ process thus is a laboratory for testing QCD color transparency.[10]

Regge behavior of structure functions. The light-cone wavefunctions $\psi_{n/H}$ of a hadron are not independent of each other, but rather are coupled via the equations of motion. Antonuccio, Dalley and I [136] have used the constraint of finite "mechanical" kinetic energy to derive "ladder relations" which interrelate the light-cone wavefunctions of states differing by one or two gluons. We then use these relations to derive the Regge behavior of both the polarized and unpolarized structure functions at $x \to 0$, extending Mueller's derivation of the BFKL hard QCD pomeron from the properties of heavy quarkonium light-cone wavefunctions at large N_C QCD.[137]

Structure functions at large x_{bj}. The behavior of structure functions where one quark has the entire momentum requires the knowledge of LC wavefunctions with $x \to 1$ for the struck quark and $x \to 0$ for the spectators. This is a highly off-shell configuration, and thus one can rigorously derive quark-counting and helicity-retention rules for the power-law behavior of the polarized and unpolarized quark and gluon distributions in the $x \to 1$ endpoint domain.

DGLAP evolution at $x \to 1$ Usually one expects that structure functions are strongly suppressed at large x because of the momentum lost by gluon radiation: the predicted change of the power law behavior at large x is[138]

$$\frac{F_2(x, Q^2)}{F_2(x, Q_0^2)} \underset{x \to 1}{=} (1-x)^{\zeta(Q^2, Q_0^2)} \tag{68}$$

where

$$\zeta(q^2, Q_0^2) = \frac{1}{4\pi} \int_{Q_0^2}^{Q^2} \frac{d\ell^2}{\ell^2} \alpha_s(\ell^2) \ . \tag{69}$$

Because of asymptotic freedom, this implies a $\log\log Q^2$ increase in the effective power $\zeta(Q^2, Q_0^2)$. However, this derivation assumes that the struck quark is on its mass shell. The off-shell effect is profound, greatly reducing the PQCD radiation.[12, 139] We can take into account the main effect of the struck quark virtuality by modifying the propagator in Eq. (69):

$$\zeta(Q^2, Q_0^2) = \frac{1}{4\pi} \int_{Q_0^2}^{Q^2} \frac{d\ell^2}{\ell^2 + |k_f^2|} \alpha_s(\ell^2). \tag{70}$$

Thus at large x, there is effectively no DGLAP evolution until $Q^2 \gtrsim |k_f^2|$! One can also see that DGLAP evolution at large x at fixed Q^2 must be suppressed in order to have duality at fixed $W^2 = Q^2(1 - x_{bj})/x_{bj}$ between the inclusive electroproduction and exclusive resonance contributions.[4] Thus evolution of structure functions is minimal in this domain because the struck quark is highly virtual as $x \to 1$; *i.e.* the starting point Q_0^2 for evolution cannot be held fixed, but must be larger than a scale of order $(m^2 + k_\perp^2)/(1 - x)$.[76, 7, 140]

Materialization of far-off-shell configurations. In a high energy hadronic collisions, the highly-virtual states of a hadron can be materialized into physical hadrons simply by the soft interaction of any of the constituents.[141] Thus a proton state with intrinsic charm $|\, uud\overline{c}c\rangle$ can be materialized, producing a J/ψ at large x_F, by the interaction of a light-quark in the target. The production occurs on the front-surface of a target nucleus, implying an $A^{2/3}$ J/ψ production cross section at large x_F, which is consistent with experiment, such as Fermilab experiments E772 and E866.

Comover phenomena. Light-cone wavefunctions describe not only the partons that interact in a hard subprocess but also the associated partons freed from the projectile. The projectile partons which are comoving (*i.e.*, which have similar rapidity) with final state quarks and gluons can interact strongly producing (a) leading particle effects, such as those seen in open charm hadroproduction; (b) suppression of quarkonium [142] in favor of open heavy hadron production, as seen in the E772 experiment; (c) changes in color configurations and selection rules in quarkonium hadroproduction, as has been emphasized by Hoyer and Peigne.[143] All of these effects violate the usual ideas of factorization for inclusive reactions. Further, more than one parton from the projectile can enter the hard subprocess, producing dynamical higher-twist contributions, as seen for example in Drell-Yan experiments.[144, 145]

Jet hadronization in light-cone QCD. One of the goals of nonperturbative analysis in QCD is to compute jet hadronization from first principles. The DLCQ solutions provide a possible method to accomplish this. By inverting the DLCQ solutions, we can write the "bare" quark state of the free theory as $|\, q_0\rangle = \sum |\, n\rangle \langle n \,|\, q_0\rangle$ where now $\{|\, n\rangle\}$ are the exact DLCQ eigenstates of H_{LC}, and $\langle n \,|\, q_0\rangle$ are the DLCQ projections of the eigensolutions. The expansion in automatically infrared and ultraviolet

regulated if we impose global cutoffs on the DLCQ basis: $\lambda^2 < \Delta\mathcal{M}_n^2 < \Lambda^2$ where $\Delta\mathcal{M}_n^2 = \mathcal{M}_n^2 - (\Sigma\mathcal{M}_i)^2$. It would be interesting to study jet hadronization at the amplitude level for the existing DLCQ solutions to QCD (1+1) and collinear QCD.

Hidden Color. The deuteron form factor at high Q^2 is sensitive to wavefunction configurations where all six quarks overlap within an impact separation $b_{\perp i} < \mathcal{O}(1/Q)$. The leading power-law fall off predicted by QCD is $F_d(Q^2) = f(\alpha_s(Q^2))/(Q^2)^5$, where, asymptotically, $f(\alpha_s(Q^2)) \propto \alpha_s(Q^2)^{5+2\gamma}$.[146] The derivation of the evolution equation for the deuteron distribution amplitude and its leading anomalous dimension γ is given in the references.[147] In general, the six-quark wavefunction of a deuteron is a mixture of five different color-singlet states. The dominant color configuration at large distances corresponds to the usual proton-neutron bound state. However at small impact space separation, all five Fock color-singlet components eventually acquire equal weight, *i.e.*, the deuteron wavefunction evolves to 80% "hidden color." [148] The relatively large normalization of the deuteron form factor observed at large Q^2 hints at sizable hidden-color contributions.[149] Hidden color components can also play a predominant role in the reaction $\gamma d \to J/\psi pn$ at threshold if it is dominated by the multi-fusion process $\gamma gg \to J/\psi$.

Nuclear Structure Functions at $1 < x_{bj} < A$, beyond the kinematic domain accessible on a single nucleon target. The nuclear light-cone momentum must be transferred to a single quark, requiring quark-quark correlations between quarks of different nucleons in a compact, far-off-shell regime. Also, as noted above, the nuclear wavefunction contains hidden-color components distinct from a convolution of separate color-singlet nucleon wavefunctions.

Spin-Spin Correlations in Nucleon-Nucleon Scattering and the Charm Threshold. One of the most striking anomalies in elastic proton-proton scattering is the large spin correlation A_{NN} observed at large angles.[150] At $\sqrt{s} \simeq 5$ GeV, the rate for scattering with incident proton spins parallel and normal to the scattering plane is four times larger than that for scattering with anti-parallel polarization. This strong polarization correlation can be attributed to the onset of charm production in the intermediate state at this energy.[151] The intermediate state $|uuduudc\bar{c}\rangle$ has odd intrinsic parity and couples to the $J = S = 1$ initial state, thus strongly enhancing scattering when the incident projectile and target protons have their spins parallel and normal to the scattering plane. The charm threshold can also explain the anomalous change in color transparency observed at the same energy in quasi-elastic pp scattering. A crucial test is the observation of open charm production near threshold with a cross section of order of 1μb.

15 Conclusions

In these lectures I have discussed how the universal, process-independent and frame-independent light-cone Fock-state wavefunctions encode the properties of a hadron in terms of its fundamental quark and gluon degrees of freedom. Given the proton's

light-cone wavefunctions, one can compute not only the moments of the quark and gluon distributions measured in deep inelastic lepton-proton scattering, but also the multi-parton correlations which control the distribution of particles in the proton fragmentation region and dynamical higher twist effects. Light-cone wavefunctions also provide a systematic framework for evaluating exclusive hadronic matrix elements, including time-like heavy hadron decay amplitudes and form factors. The formalism also provides a physical factorization scheme for separating hard and soft contributions in both exclusive and inclusive hard processes. I have discussed a number of applications of light-cone Fock representation of QCD, including semileptonic B decays, deeply virtual Compton scattering, and dynamical higher twist effects in inclusive reactions. The relation of the intrinsic sea to the light-cone wavefunctions is discussed. The physics of light-cone wavefunctions is illustrated for the quantum fluctuations of an electron. A new type of jet production reaction, "self-resolving diffractive interactions" can provide direct information on the light-cone wavefunctions of hadrons in terms of their QCD degrees of freedom, as well as the composition of nuclei in terms of their nucleon and mesonic degrees of freedom. I have also reviewed the strong progress that has been made in computing light-cone wavefunctions directly from the QCD light-cone Hamiltonian. Even without full non-perturbative solutions of QCD, one can envision a program to construct the light-cone wavefunctions using measured moments constraints from QCD sum rules, lattice gauge theory, hard exclusive and inclusive processes. One is guided by theoretical constraints from perturbation theory which dictates the asymptotic form of the wavefunctions at large invariant mass, $x \to 1$, and high $k_\perp$. One can also use constraints from ladder relations which connect Fock states of different particle number; perturbatively-motivated numerator spin structures; conformal symmetry, guidance from toy models such as "reduced" $QCD(1+1)$; and the correspondence to Abelian theory for $N_C \to 0$, and the many-body Schrödinger theory in the nonrelativistic domain.

Acknowledgments

Work supported by the Department of Energy under contract number DE-AC03-76SF00515. I wish to thank Fernando Navarra and Martina Nielson for their kind hospitality in Brazil. Much of this work is based on collaborations, particularly with Markus Diehl, Paul Hoyer, Dae Sung Hwang, Peter Lepage, Bo-Qiang Ma, Hans Christian Pauli, Johan Rathsman, Ivan Schmidt, and Prem Srivastava.

References

[1] H. Fritzsch, M. Gell-Mann and H. Leutwyler, Phys. Lett. **B47**, 365 (1973).

[2] P. A. Dirac, Rev. Mod. Phys. **21**, 392 (1949).

[3] For a review of light-cone methods and further references see S. J. Brodsky, H. Pauli, and S. S. Pinsky, Phys. Rept. **301**, 299 (1998).

[4] The notation and calculational rules for light-cone perturbation theory can be found in: G. P. Lepage and S. J. Brodsky, Phys. Rev. **D 22**, 2157 (1980); Phys. Lett. **B 87**, 359 (1979); Phys. Rev. Lett. **43**, 545, 1625(E) (1979).

[5] S. J. Brodsky, *Light-Cone Quantized QCD and Novel Hadron Phenomenology*, SLAC-PUB-7645, 1997; S. J. Brodsky and H. C. Pauli, *Light-Cone Quantization and QCD*, Lecture Notes in Physics, vol. 396, eds., H. Mitter *et al.*, Springer-Verlag, Berlin, 1991; S. J. Brodsky, H. Pauli and S. S. Pinsky, Phys. Rept. **301**, 299 (1998).

[6] P. P. Srivastava and S. J. Brodsky, Phys. Rev. **D61**, 025013 (2000), hep-ph/9906423, and SLAC-PUB 8543, in preparation.

[7] S. J. Brodsky and G. P. Lepage, in *Perturbative Quantum Chromodynamics*, A. H. Mueller, Ed. (World Scientific, 1989).

[8] S. J. Brodsky, D. S. Hwang, B. Ma and I. Schmidt, hep-th/0003082.

[9] R. L. Jaffe and A. Manohar, Nucl. Phys. **B321**, 343 (1989).

[10] S. J. Brodsky and A. H. Mueller, Phys. Lett. **206B**, 685 (1988); L. Frankfurt and M. Strikman, Phys. Rept. **160**, 235 (1988); P. Jain, B. Pire and J. P. Ralston, Phys. Rept. **271**, 67 (1996).

[11] O. Nachtmann, Nucl. Phys. **B63**, 237 (1973).

[12] S. J. Brodsky and G. P. Lepage, SLAC-PUB-2447 *Presented at Summer Institute on Particle Physics, SLAC, Stanford, Calif., Jul 9-20, 1979.*

[13] D. Ashery [E791 Collaboration], hep-ex/9910024.

[14] S. J. Brodsky, Y. Frishman, G. P. Lepage and C. Sachrajda, *Phys. Lett.* **91B**, 239 (1980).

[15] D. Müller, *Phys. Rev.* **D49**, 2525 (1994).

[16] V. M. Braun, S. E. Derkachov, G. P. Korchemsky and A. N. Manashov, Nucl. Phys. **B553**, 355 (1999), hep-ph/9902375.

[17] S. J. Brodsky and H. J. Lu, *Phys. Rev.* **D51**, 3652 (1995), hep-ph/9405218.

[18] S. J. Brodsky, J. R. Pelaez and N. Toumbas, Phys. Rev. **D60**, 037501 (1999), hep-ph/9810424.

[19] S. J. Brodsky, G. T. Gabadadze, A. L. Kataev and H. J. Lu, *Phys. Lett.* **B372**, 133 (1996) hep-ph/9512367.

[20] S. J. Brodsky and J. Rathsman, hep-ph/9906339.

[21] S. J. Brodsky, E. Gardi, G. Grunberg and J. Rathsman, hep-ph/0002065.

[22] S. J. Brodsky, M. S. Gill, M. Melles, and J. Rathsman, Phys. Rev. **D58**, 116006 (1998).

[23] S. J. Brodsky and P. Huet, Phys. Lett. **B417**, 145 (1998), hep-ph/9707543.

[24] S. J. Brodsky, hep-ph/9912340.

[25] S. D. Drell and T. Yan, Phys. Rev. Lett. **24**, 181 (1970).

[26] G. B. West, Phys. Rev. Lett. **24**, 1206 (1970).

[27] For a review and further references see S. J. Brodsky, H. Pauli and S. S. Pinsky, Phys. Rept. **301**, 299 (1998), hep-ph/9705477.

[28] S. J. Brodsky and D. S. Hwang, Nucl. Phys. **B543**, 239 (1999), hep-ph/9806358.

[29] C. R. Ji and H. M. Choi, Fizika **B8**, 321 (1999).

[30] S. J. Brodsky, M. Diehl, and D. S. Hwang, in preparation.

[31] S. J. Brodsky and S. D. Drell, Phys. Rev. **D 22**, 2236 (1980).

[32] S. D. Drell and T. M. Yan, Phys. Rev. Lett. **24**, 181 (1970).

[33] X.-S. Chen, D. Qing, and F. Wang, Chin. Phys. Lett. **16**, 403 (1999), hep-ph/9802347; D. Qing, X.-S. Chen, and F. Wang, Phys. Rev. **D 58**, 114032 (1998).

[34] S. J. Brodsky and F. Schlumpf, Phys. Lett. **B 329**, 111 (1994).

[35] X. Ji, Talk presented at 12th Int. Symp. on High-Energy Spin Physics (SPIN96), Amsterdam, Sep. 1996, hep-ph/9610369; Phys. Rev. Lett. **78** (1997) 610; Phys. Rev. **D 55**, 7114 (1997).

[36] S. J. Brodsky and S. D. Drell, Phys. Rev. **D22**, 2236 (1980).

[37] A. Harindranath and R. Kundu, Phys. Rev. **D59**, 116013 (1999), hep-ph/9802406.

[38] L. Okun and I. Yu. Kobzarev, ZhETF, **43** 1904 (1962) (English translation : JETP **16** 1343 (1963)); L. Okun, in proceedings of the International Conference on Elementary Particles, 4th, Heidelberg, Germany (1967). Edited by H. Filthuth. North-Holland, (1968).

[39] X. Ji, hep-ph/9610369.

[40] X. Ji, Phys. Rev. Lett. **78**, 610 (1997), hep-ph/9603249.

[41] X. Ji, Phys. Rev. **D55**, 7114 (1997), hep-ph/9609381.

[42] O. V. Teryaev, hep-ph/9904376.

[43] B.-Q. Ma, J. Phys. **G 17** (1991) L53; B.-Q. Ma and Q.-R. Zhang, Z. Phys. **C 58**, 479 (1993).

[44] B.-Q. Ma and I. Schmidt, Phys. Rev. **D 58**, 096008 (1998).

[45] P. Hägler and A. Schäfer, Phys. Lett. **B 430**, 179 (1998).

[46] F. E. Close, Phys. Lett. **B 43**, 422 (1973).

[47] S. J. Brodsky and J. R. Hiller, Phys. Rev. **D 46**, 2141 (1992).

[48] S. J. Brodsky, J. R. Hiller and G. McCartor, Phys. Rev. **D58**, 025005 (1998), hep-th/9802120.

[49] P. V. Landshoff, J C. Polkinghorne and R. D. Short, Nucl. Phys. **B 28**, 225 (1971).

[50] S. J. Brodsky, F. E. Close, and J. F. Gunion, Phys. Rev. **D 8**, 3678 (1973).

[51] B.-Q. Ma, Phys. Lett. **B 375**, 320 (1996).

[52] B.-Q. Ma, I. Schmidt, and J. Soffer, Phys. Lett. **B 441**, 461 (1998).

[53] S. J. Brodsky, F. E. Close, and J. F. Gunion, Phys. Rev. **D 5**, 1384 (1972); Phys. Rev. **D 6**, 177 (1972); Phys. Rev. **D 8**, 3678 (1973).

[54] M. Diehl, T. Gousset, and B. Pire, hep-ph/0003233.

[55] X. Ji, Talk presented at 12th Int. Symp. on High-Energy Spin Physics (SPIN96), Amsterdam, Sep. 1996, hep-ph/9610369; Phys. Rev. Lett. **78**, 610 (1997); Phys. Rev. **D 55**, 7114 (1997).

[56] X. Ji, J. Phys. **G 24**, 1181 (1998), hep-ph/9807358.

[57] A. V. Radyushkin, Phys. Lett. **B 380**, 417 (1996), hep-ph/960431; Phys. Rev. **D 56**, 5524 (1997), hep-ph/9704207.

[58] X. Ji and J. Osborne, Phys. Rev. **D 58**, 094018 (1998), hep-ph/9801260.

[59] P. A. Guichon and M. Vanderhaeghen, Prog. Part. Nucl. Phys. **41**, 125 (1998), hep-ph/9806305.

[60] M. Vanderhaeghen, P. A. Guichon, and M. Guidal, Phys. Rev. Lett. **80**, 5064 (1998).

[61] A. V. Radyushkin, Phys. Rev. **D 59**, 014030 (1999), hep-ph/9805342.

[62] J. C. Collins and A. Freund, Phys. Rev. **D 59**, 074009 (1999), hep-ph/9801262.

[63] M. Diehl, T. Feldmann, R. Jakob, and P. Kroll, Eur. Phys. J. **C 8**, 409 (1999), hep-ph/9811253.

[64] M. Diehl, T. Feldmann, R. Jakob and P. Kroll, Phys. Lett. **B460**, 204 (1999), hep-ph/9903268.

[65] J. Blumlein and D. Robaschik, hep-ph/0002071.

[66] D. Muller, D. Robaschik, B. Geyer, F. M. Dittes and J. Horejsi, Fortsch. Phys. **42**, 101 (1994) [hep-ph/9812448].

[67] S. J. Brodsky and D. S. Hwang, Nucl. Phys. **B 543**, 239 (1999).

[68] S. J. Chang, R. G. Root and T. M. Yan, Phys. Rev. **D 7**, 1133 (1973).

[69] M. Burkardt, Nucl. Phys. **A 504** (1989) 762; Nucl. Phys. **B 373**, 613 (1992); Phys. Rev. **D 52**, 3841 (1995).

[70] H.-M. Choi and C.-R. Ji, Phys. Rev. **D 58**, 071901 (1998).

[71] K. Hornbostel, S. J. Brodsky, and H. C. Pauli, *Phys. Rev.* **D41**, 3814 (1990).

[72] F. Antonuccio and S. Dalley, *Phys. Lett.* **B348**, 55 (1995); *Phys. Lett.* **B376**, 154 (1996); *Nucl. Phys.* **B461**, 275 (1996).

[73] G. P. Lepage and S. J. Brodsky, Phys. Rev. **D22**, 2157 (1980).

[74] G. P. Lepage and S. J. Brodsky, Phys. Lett. **B 87**, 359 (1979).

[75] S. D. Bass, S. J. Brodsky and I. Schmidt, Phys. Rev. **D60**, 034010 (1999), hep-ph/9901244.

[76] G. P. Lepage and S. J. Brodsky, Phys. Rev. **D22**, 2157 (1980); Phys. Lett. **B87**, 359 (1979); Phys. Rev. Lett. **43**, 545, 1625(E) (1979).

[77] S. J. Brodsky, C.-R. Ji, A. Peng and D. G. Robertson, Phys. Rev. **D57**, 345 (1998).

[78] G. P. Lepage and S. J. Brodsky, Phys. Rev. Lett. **43**, 545 (1979).

[79] A. Szczepaniak, E. M. Henley and S. J. Brodsky, Phys. Lett. **B243**, 287 (1990).

[80] M. Beneke, G. Buchalla, M. Neubert and C. T. Sachrajda, hep-ph/9905312.

[81] A. Szczepaniak, Phys. Rev. **D54**, 1167 (1996).

[82] P. Ball and V. M. Braun, Phys. Rev. **D58**, 094016 (1998) hep-ph/9805422.

[83] H. C. Pauli and S. J. Brodsky, Phys. Rev. **D32**, 2001 (1985).

[84] S. Dalley and I. R. Klebanov, Phys. Rev. **D47**, 2517 (1993), hep-th/9209049.

[85] S. Dalley, and I. R. Klebanov, Phys. Rev. **D47**, 2517 (1993).

[86] S. J. Brodsky, J. R. Hiller and G. McCartor, Phys. Rev. **D60**, 054506 (1999), hep-ph/9903388.

[87] S. Dalley and B. van de Sande, hep-lat/9911035, and S. Dalley (to be published).

[88] J. R. Hiller and S. J. Brodsky, Phys. Rev. **D59**, 016006 (1999), hep-ph/9806541.

[89] P. P. Srivastava and S. J. Brodsky, hep-ph/9906423.

[90] F. Antonuccio, I. Filippov, P. Haney, O. Lunin, S. Pinsky, U. Trittmann and J. Hiller [SDLCQ Collaboration], hep-th/9910012.

[91] O. Lunin and S. Pinsky, hep-th/9910222.

[92] P. Haney, J. R. Hiller, O. Lunin, S. Pinsky and U. Trittmann, hep-th/9911243.

[93] A. Bassetto, L. Griguolo and F. Vian, hep-th/9911036.

[94] K. Yamawaki, hep-th/9802037.

[95] S. S. Pinsky and B. van de Sande, Phys. Rev. **D49**, 2001 (1994), hep-ph/9310330.

[96] G. Bertsch, S. J. Brodsky, A. S. Goldhaber, and J. F. Gunion, Phys. Rev. Lett. **47**, 297 (1981).

[97] L. Frankfurt, G. A. Miller, and M. Strikman, Phys. Lett. **B304**, 1 (1993), hep-ph/9305228.

[98] L. Frankfurt, G. A. Miller and M. Strikman, hep-ph/9907214.

[99] S. Brodsky, M. Diehl, P. Hoyer, and S. Peigne, in preparation.

[100] J. Gronberg *et al.* [CLEO Collaboration], Phys. Rev. **D57**, 33 (1998), hep-ex/9707031.

[101] P. Stoler, Few Body Syst. Suppl. **11**, 124 (1999).

[102] G. A. Miller, nucl-th/9910053.

[103] G. A. Miller, S. J. Brodsky and M. Karliner, hep-ph/0002156.

[104] M. Virchaux and A. Milsztajn, Phys. Lett. **B274**, 221 (1992).

[105] P. Amaudruz *et al.* [New Muon Collaboration], Nucl. Phys. **B371**, 3 (1992).

[106] M. Beneke, Phys. Rept. **317**, 1 (1999), hep-ph/9807443.

[107] M. Maul, E. Stein, A. Schafer and L. Mankiewicz, Phys. Lett. **B401**, 100 (1997), hep-ph/9612300.

[108] P. A. Souder, "Higher Twist and Parity", these proceedings.

[109] S. J. Brodsky, G. P. Lepage and P. B. Mackenzie, Phys. Rev. **D28**, 228 (1983).

[110] E. D. Bloom and F. J. Gilman, Phys. Rev. Lett. **25**, 1140 (1970).

[111] R. Blankenbecler, S. J. Brodsky and J. F. Gunion, Phys. Rev. **D18**, 900 (1978); S. J. Brodsky, J. F. Gunion, and M. Scadron (unpublished).

[112] M. Guanziroli *et al.* [NA10 Collaboration], Z. Phys. **C37**, 545 (1988).

[113] J. S. Conway *et al.*, Phys. Rev. **D39**, 92 (1989).

[114] E. L. Berger and S. J. Brodsky, Phys. Rev. Lett. **42**, 940 (1979).

[115] A. Brandenburg, S. J. Brodsky, V. V. Khoze and D. Muller, Phys. Rev. Lett. **73**, 939 (1994), hep-ph/9403361.

[116] C. Biino *et al.*, Phys. Rev. Lett. **58**, 2523 (1987).

[117] M. Vanttinen, P. Hoyer, S. J. Brodsky and W. K. Tang, Phys. Rev. **D51**, 3332 (1995), hep-ph/9410237.

[118] S. J. Brodsky, P. Hoyer, C. Peterson and N. Sakai, Phys. Lett. **B93**, 451 (1980).

[119] B. W. Harris, J. Smith and R. Vogt, Nucl. Phys. **B461**, 181 (1996), hep-ph/9508403.

[120] S. J. Brodsky, P. Hoyer, and J. M. Laget, in preparation.

[121] S. D. Drell, SLAC-PUB-5720 *Presented at the 1991 SLAC Summer Institute on Particle Physics: Lepton Hadron Scattering, Stanford, CA, Aug 5-16, 1991.*

[122] See *e.g.*, S. Capitani *et al.*, hep-lat/9908038, and references therein.

[123] J. Edelmann, G. Piller, N. Kaiser and W. Weise, Nucl. Phys. **A665**, 125 (2000) [hep-ph/9909524].

[124] P. Castorina and P. J. Mulders, Phys. Rev. **D31**, 2760 (1985).

[125] S. J. Brodsky, G. P. Lepage and S. A. Zaidi, Phys. Rev. **D23**, 1152 (1981).

[126] M. Franz, M. V. Polyakov and K. Goeke, hep-ph/0002240.

[127] S. J. Brodsky, C. Peterson and N. Sakai, Phys. Rev. **D23**, 2745 (1981).

[128] S. J. Brodsky and I. A. Schmidt, Phys. Lett. **B234**, 144 (1990).

[129] S. J. Brodsky and M. Karliner, Phys. Rev. Lett. **78**, 4682 (1997), hep-ph/9704379.

[130] S. J. Brodsky, G. P. Lepage and S. F. Tuan, Phys. Rev. Lett. **59**, 621 (1987).

[131] S. J. Brodsky and G. P. Lepage, Phys. Rev. **D24**, 2848 (1981).

[132] M. Burkardt and Brian Warr, *Phys. Rev.* **D45**, 958 (1992).

[133] A. I. Signal and A. W. Thomas, *Phys. Lett.* **191B**, 205 (1987).

[134] S. J. Brodsky and B.-Q. Ma, *Phys. Lett.* **B381**, 317 (1996), hep-ph/9604393.

[135] S. J. Brodsky, L. Frankfurt, J. F. Gunion, A. H. Mueller, and M. Strikman, *Phys. Rev.* **D50**, 3134 (1994), hep-ph/9402283.

[136] F. Antonuccio, S. J. Brodsky, and S. Dalley, Phys. Lett. **B412**, 104 (1997), hep-ph/9705413.

[137] A. H. Mueller, Phys. Lett. **B308**, 355 (1993).

[138] V. N. Gribov and L. N. Lipatov, Yad. Fiz. **15**, 781 (1972).

[139] G. P. Lepage, S. J. Brodsky, T. Huang and P. B. Mackenzie, CLNS-82/522, published in Banff Summer Inst.1981:0083 (QCD161:B23:1981); S. J. Brodsky, T. Huang and G. P. Lepage, *In *Banff 1981, Proceedings, Particles and Fields 2*, 143-199.*

[140] D. Mueller, SLAC-PUB-6496, May 1994, hep-ph/9406260.

[141] S. J. Brodsky, P. Hoyer, A. H. Mueller, W.-K. Tang, *Nucl. Phys.* **B369**, 519 (1992).

[142] See Brodsky and Mueller[10]. R. Vogt, S. J. Brodsky, and P. Hoyer, Nucl. Phys. **B360**, 67 (1991); Nucl. Phys. **B383**, 643 (1992).

[143] P. Hoyer and S. Peigne, Phys. Rev. **D59**, 034011 (1999), hep-ph/9806424.

[144] E. L. Berger and S. J. Brodsky, Phys. Rev. Lett. **42**, 940 (1979).

[145] A. Brandenburg, S. J. Brodsky, V.V. Khoze, and D. Mueller, Phys. Rev. Lett. **73**, 939 (1994), hep-ph/9403361.

[146] S. J. Brodsky and B. T. Chertok, Phys. Rev. **D14**, 3003 (1976).

[147] S. J. Brodsky, C.-R. Ji, and G. P. Lepage, Phys. Rev. Lett. **51**, 83 (1983).

[148] S. J. Brodsky, C. Ji and G. P. Lepage, Phys. Rev. Lett. **51**, 83 (1983).

[149] G. R. Farrar, K. Huleihel and H. Zhang, Phys. Rev. Lett. **74**, 650 (1995).

[150] A. D. Krisch, Nucl. Phys. B (Proc. Suppl.) **25**, 285 (1992).

[151] S. J. Brodsky and G. F. de Teramond, Phys. Rev. Lett. **60**, 1924 (1988).